Energy Management of Grid Interconnected Multi-Microgrids Based on P2P Energy Exchange: A Data Driven Approach

Kannan Thirugnanam [ID], *Member, IEEE*, Mohamed Shawky El Moursi [ID], *Senior Member, IEEE*, Vinod Khadkikar [ID], *Senior Member, IEEE*, Hatem H. Zeineldin [ID], *Senior Member, IEEE*, and Mohamed Al Hosani [ID], *Senior Member, IEEE*

Abstract—Grid interconnected multi-microgrids provides potential benefits to the consumers, where the microgrids (MGs) equipped with distributed generators (DGs), energy storage systems (ESSs), and diesel generators. However, intermittency of DGs, high cost of ESSs, and depleting fossil fuels are the major challenges for the economic operation of interconnected multi-microgrids. One potential way to address these challenges is to develop an energy management strategy (EMS) for the grid interconnected multi-microgrids. This paper proposes an EMS to reduce consumer energy consumption cost (ECC) using fuzzy-based peer-to-peer (P2P) energy exchange algorithm with dynamic pricing. In this context, the MGs consumers load power demand (LPD) and DGs output behaviors are modeled using random vector functional link network approach to predict future time slot values. Then, a fuzzy-based P2P energy exchange algorithm is developed to enable the surplus energy transfer to grid and/or MGs with dynamic pricing. Furthermore, an ESS charging/discharging energy control and diesel generator turn ON strategies are developed based on the MGs deficit power. Then, the MGs consumer LPD reduction strategy is implemented based on the consumer ECC margin and energy consumption index. Finally, an EMS is proposed that includes on demand-supply strategy and consumer energy consumption cost reduction strategy based on the future time slot values. The novelty of the proposed work lies within the energy management of grid interconnected multi-microgrids and the reduction of consumers ECC through surplus energy transfer to grid and/or MGs using fuzzy-based P2P energy exchange algorithm with dynamic pricing. Historical data are used to demonstrate the effectiveness of the proposed EMS for grid interconnected multi-microgrids.

Index Terms—Deep neural network, distributed generators, energy management, energy storage, fuzzy logic, microgrids, and peer-to-peer energy exchange.

Kannan Thirugnanam is with the Department of Electrical and Computer Science, Khalifa University of Science and Technology, Abu Dhabi 127788, UAE (e-mail: kannan.thirugnanam.phd@ieee.org).

Mohamed Shawky El Moursi is with the Advanced Power and Energy Center (APEC), Department of Electrical Engineering and Computer Science, Khalifa University, Abu Dhabi 127788, UAE, on leave from the Faculty of Engineering, Mansoura University, Mansoura 35516, Egypt (e-mail: mohamed.elmoursi@ku.ac.ae).

Vinod Khadkikar is with the Advanced Power and Energy Center (APEC), Department of Electrical Engineering and Computer Science, Khalifa University of Science and Technology, Abu Dhabi 127788, UAE (e-mail: vkhadkikar@ku.ac.ae).

Hatem H. Zeineldin is with the Faculty of Engineering, Cairo University, Giza 12613, Egypt, on leave from Khalifa University of Science and Technology, Abu Dhabi 127788, UAE, (e-mail: hatem.zeineldin@ku.ac.ae).

Mohamed Al Hosani is with the Department of Demand Side Management, Abu Dhabi Distribution Company, Abu Dhabi 219, UAE (e-mail: malhosani85@hotmail.com).

Color versions of one or more of the figures in this article are available online at https://ieeexplore.ieee.org.

Digital Object Identifier 10.1109/TPWRS.2020.3025113

NOMENCLATURE

h, m, H	Present time slot, future time slot, and total number of time slots (minutes).
i, I	Microgrids and total number of microgrids.
Coefficients	
a_i, b_i, c_i	Regression coefficients.
$a_{e,i}, b_{e,i}$	Charge rate coefficients of ith MG.
$c_{e,i}, d_{e,i}$	Discharge rate coefficients of ith MG.
Constants	
A_t, A_p	Air temperature and pressure ($^\circ$C, J/m^3).
$\mathrm{I}^0_{ec,i}$	Initial value of consumer energy consumption index of ith MG.
$SOC^{in}_{e,i}$	Initial state-of-charge of ith MG (%).
$\mathrm{S}_{e,i}$	Energy storage system size of ith MG (kWh).
$\Delta h, \hbar$	Time slot difference and sum of present and future time slot, i.e $\hbar = h + m$ (minutes).
$\eta_{c,i}, \eta_{e,i}$	Converter and ESS efficiency of ith MG (%).
$\eta_{d,i}$	Diesel generator efficiency of ith MG (%).
w^z_j	Weight of jth enhancement node.
Limits	
b^z_j	Threshold limits for consumer LPD, solar PV power, and wind turbine power.
$C^{max}_{e,i}$	Maximum charge rate limit of ith MG (1/hour).
$D^{max}_{e,i}$	Maximum discharge rate limit of ith MG (1/hour).
$D^{max}_{d,i}$	Diesel generator maximum turned ON duration of ith MG (hour).
$\mathrm{I}^{max}_{ec,i}$	Maximum consumer energy consumption index of ith MG.
$P^{max}_{l,i}$	Maximum consumer LPD of ith MG (kW).

$P_{sr,i}^{max}$ — Maximum surplus power of ith MG at time slot $\hbar$ (kW).

$\mathcal{E}_{con,i}^{max}$ — Maximum electricity consumption of ith MG (kWh).

$\mathbb{E}_{cost,i}^{max,\hbar}$ — Maximum threshold limit for consumer ECC of ith MG at time slot $\hbar$ (S\$/kWh).

$\mathbb{E}_{cost,i}^{min,\hbar}$ — Minimum threshold limit for consumer ECC of ith MG at time slot $\hbar$ (S\$/kWh).

$\mathrm{I}_{ec,i}^{min}$ — Minimum threshold limit for consumer energy consumption index of ith MG.

Power and Energy Cost

$P_{e,i}^h$ — Charging and discharging power of ith MG at time slot h (kW).

$P_{e,i}^h\{c\}$ — Charging power of ith MG at time slot h (kW).

$P_{e,i}^h\{d\}$ — Discharging power of ith MG at time slot h (kW).

$P_{d,i}^r, P_{d,i}^h$ — Diesel generator rated power and output power of ith MG at time slot h (kW).

$P_{df,i}^\hbar, P_{sr,i}^\hbar$ — Deficit and surplus power of ith MG at time slot $\hbar$ (kW).

$P_{dg,i}^\hbar$ — Sum of solar PV and wind turbine output power of ith MG at time slot $\hbar$ (kW).

$P_{ld,i}^\hbar$ — Sum of predicted consumer load power demand and power loss of ith MG at time slot $\hbar$ (kW).

$P_{loss,i}^\hbar$ — Power loss of ith MG at time slot $\hbar$ (kW).

$P_{pv,i}^r, P_{wt,i}^r$ — Solar PV and wind turbine rated power of ith MG (kW).

$\mathcal{P}_{b,g}^{\hbar,*}, \mathcal{P}_{s,g}^{\hbar,*}$ — Buying and selling power reference signal of grid at time slot $\hbar$ (kW).

$\mathcal{P}_{b,i}^{\hbar,*}, \mathcal{P}_{s,i}^{\hbar,*}$ — Buying and selling power reference signal of ith MG at time slot $\hbar$ (kW).

$E_{e,i}^h\{c\}$ — Charging energy of ith MG at time slot h (kWh).

$E_{e,i}^h\{d\}$ — Discharging energy of ith MG at time slot h (kWh).

$E_{d,i}^h, E_{d,i}^{h,*}$ — Diesel generator energy and reference signal of ith MG at time slot h (kWh).

$\mathcal{E}_{con,i}^\hbar$ — Total electricity consumption of ith MG at time slot $\hbar$ (kWh).

$\mathcal{E}_{df,i}^\hbar, \mathcal{E}_{sr,i}^\hbar$ — Deficit and surplus energy of ith MG at time slot $\hbar$ (kWh).

$\mathcal{E}_{p2p}^{\hbar,*}$ — Peer-to-peer energy exchange reference signal at time slot $\hbar$ (kWh).

$\mathcal{E}_{p2p,i}^{\hbar,*}$ — Peer-to-peer energy exchange reference signal of ith MG at time slot $\hbar$ (kWh).

$\mathcal{E}_{p2p,g}^{\hbar,*}$ — Peer-to-peer energy exchange reference signal of grid at time slot $\hbar$ (kWh).

$\mathbb{B}_{cost,i}^\hbar$ — Energy buying cost of ith MG at time slot $\hbar$ (S\$/kWh).

$\mathbb{C}_{b,i}^{\hbar,*}, \mathbb{C}_{s,i}^{\hbar,*}$ — Buying and selling energy cost reference signal of ith MG at time slot $\hbar$ (S\$/kWh).

$\mathbb{C}_{b,g}^{\hbar,*}, \mathbb{C}_{s,g}^{\hbar,*}$ — Buying and selling energy cost reference signal of grid at time slot $\hbar$ (S\$/kWh).

$\mathbb{C}_{d,i}^h, \mathbb{C}_{d,i}^{in}$ — Diesel generator power generation and initial cost of ith MG at time slot h (S\$/kWh).

$\mathbb{C}_i^\hbar, \mathbb{C}_{dp}^h$ — Electricity price of ith MG at time slot $\hbar$ and dynamic electricity price at time slot h (S\$/kWh).

$\mathbb{C}_{e,i}^h, \mathbb{C}_{fc}$ — ESS energy cost of ith MG at time slot h and diesel generator fuel cost (S\$/kWh).

$\mathbb{C}_{pv,i}^\hbar, \mathbb{C}_{wt,i}^\hbar$ — Solar PV and wind turbine power generation cost of ith MG at time slot $\hbar$ (S\$/kWh).

$\mathbb{C}_{p2p}^{\hbar,*}$ — Peer-to-peer energy exchange cost reference signal at time slot $\hbar$ (S\$/kWh).

$\mathbb{C}_{p2p,i}^{\hbar,*}$ — Peer-to-peer energy exchange cost reference signal of ith MG at time slot $\hbar$ (S\$/kWh).

$\mathbb{C}_{p2p,g}^{\hbar,*}$ — Peer-to-peer energy exchange cost reference signal of grid at time slot $\hbar$ (S\$/kWh).

$\mathbb{C}_{sav,i}$ — Consumer energy consumption cost savings over the ODSS and CCRS (%).

$\mathbb{C}_{tot,i}$ — Total energy consumption cost of ith MG (S\$).

$\mathbb{C}_{tot,i}^{ODSS}$ — Consumer energy consumption cost savings over the ODSS (S\$).

$\mathbb{C}_{tot,i}^{CCRS}$ — Consumer energy consumption cost savings over the CCRS (S\$).

$\mathbb{E}_{cost,i}^\hbar$ — Total energy consumption cost of ith MG at time slot $\hbar$ (S\$/kWh).

$\mathbb{S}_{cost,i}^\hbar$ — Energy selling cost of ith MG at time slot $\hbar$ (S\$/kWh).

Variables

$\mathrm{C}_{br,g}^\hbar, \mathrm{C}_{br,i}^\hbar$ — Grid circuit breaker at time slot $\hbar$ and i^{th} MG circuit breaker at time slot $\hbar$.

$F_{con,i}$ — Diesel generator fuel consumption per kWh (Liter/kWh).

h_{in}, h_{fi} — Initial and final time slot values (minutes).

$SOC_{e,i}^h$ — State-of-charge of ith MG at time slot h (%).

T_{od}, H_r — Outdoor temperature and humidity (°C, %).

x_{in}^z — Inputs for consumer LPD, solar PV power, and wind turbine power prediction model.

β_j^z, D_w — RVFLN weights and wind direction.

Control Parameters

$C_{e,i}^h, D_{e,i}^h$ — Charge and discharge rate of ith MG at time slot h (1/hour).

$\mathrm{I}_{ec,i}^\hbar$ — Consumer energy consumption index of ith MG at time slot $\hbar$.

$\mathrm{M}_{ecc,i}^\hbar$ — Consumer energy consumption cost margin of ith MG at time slot $\hbar$.

$\mathrm{UIN}_i^\hbar, \mathcal{R}_i^\hbar$ — Unique identity number and reliability index of ith MG at time slot $\hbar$.

$\mathcal{D}_{d,i}^{h,*}$ — Diesel generator turned ON duration reference signal of ith MG at time slot h (hour).

$\mathcal{K}_{d,i}^{h,*}$ — Diesel generator output power control variable reference signal of ith MG at time slot h.

$\alpha, \delta_{ec,i}$ — Objective balancing variable and error tolerance for energy consumption index of ith MG.

Prediction Parameters

$P_{l,i}^\hbar$ — Predicted consumer load power demand of ith MG at time slot $\hbar$ (kW).

$P_{pv,i}^{\hbar}, P_{wt,i}^{\hbar}$	Predicted solar PV and wind turbine output power of ith MG at time slot $\hbar$ (kW).

Forecasted/historical Parameters

$I_s^{f,h}, V_w^{f,h}$	Forecasted solar irradiance and wind velocity at time slot h (kWh/m^2, m/sec)
$T_{pv,i}^{f,h}$	Forecasted solar PV panel temperature of ith MG at time slot h (°C).
$P_{pv,i}^{f,h}, P_{wt,i}^{f,h}$	Forecasted solar PV and wind turbine output power of ith MG at time slot h (kW).
$P_{l,i}^{m,h}$	Measured consumer load power demand of ith MG at time slot $\hbar$ (kW).

I. INTRODUCTION

WITH the increased penetration of distributed generators (DGs) into the grid, interconnected multi-microgrids (IMMGs) represent one of the promising solutions for system operations [1], [2]. Also, the IMMGs received great attention for grid integration with DGs and to overcome the grid weaknesses [3]. In general, DGs, i.e., solar photovoltaic (PV) and wind turbine, with energy storage systems (ESSs) are the most feasible configuration for the IMMGs operations due to shifting the peak load demand, storing the surplus energy, mitigating the intermittency, and improving the system stability [4]. Nevertheless, frequent and inappropriate charging/discharging rate significantly reduce the ESS lifetime [5]. In addition, the consumer load power demand (LPD) is always stochastic in nature with respect to time [6]. Thus, to supply the required LPD, the IMMGs operator can utilize diesel generators to ensure higher operational flexibility [5]. In this regard, the ESS and diesel generator can be a proper combination for surplus energy storage and better operation of IMMGs [5]–[8]. However, the enhanced operation of IMMGs with diesel generator may not be a suitable solution to reduce consumer energy consumption cost (ECC) due to the major drawbacks such as high fossil fuel cost, high maintenance and operating cost, and increased environmental concerns [8]. Therefore, DGs with ESS and diesel generator may not be straightforward solutions for the cost reduction problem. Given this context, one potential way to address the consumer ECC reduction through the development of an energy management strategy (EMS), which enables the surplus energy transfer to grid and/or microgrids (MGs) through fuzzy-based peer-to-peer (P2P) energy exchange algorithm with dynamic pricing and MGs future information.

The EMS for interconnected multi-microgrids is receiving significant research interest over the past few years [1], [2]. In particular, existing work determine the total energy cost of the conventional energy drawn from the grid over a finite horizon by jointly optimizing the ESS energy subject to practical load and storage constraints [6], [7]. In [9], power/energy management schemes and an energy scheduling algorithm have been developed for a hybrid ac/dc, stand-alone, and small-scale MGs. Moreover, an EMS has been developed for the robust MGs operation based on the robust MGs operation based on the forecasting future information [10]. To maintain system robustness at minimum operational cost, a two-layer predictive EMS has been developed for MGs with hybrid ESS [11]. To

manage frequency trips due to load and renewable fluctuations, a robust EMS has been implemented for islanded MGs [12]. A general framework has been developed for reliability assessment of multi-microgrid [13]. In [14], a comprehensive control, power management system, and reinforcement learning framework has been introduced for both grid-connected and MGs operations. In addition, an energy storage dispatch and sharing methodology have been developed to reduce electricity costs for grid-connected MGs [15]. An adaptive voltage and frequency control have been developed for inverter-based DGs in a multi-microgrid structure [16]. To improve the local balance of energy generation and consumption, a hierarchical architecture has been developed and validated to identify the key elements involved in P2P energy trading [17]. Also, Paudel *et al.* implemented a novel game-theoretic model for P2P energy trading among the prosumers in a community [18]. A control strategy has been developed in [19] to match the source and load changes using P2P energy transfer. The impact of P2P energy trading among the smart [20], [21]. A two-stage aggregated control has been developed in [22], which realizes P2P energy sharing in community MGs. An optimal voltage regulation method has been developed for multi-MGs based on the multi-agent systems [23]. A P2P energy sharing mechanism has been implemented for increasing the connection of distributed energy resources based on the multi-agent framework [20].

From the literature survey, none of the previous works have considered the P2P energy exchange algorithm with dynamic pricing for consumer ECC reduction using MGs prediction models. The existing studies assume simple models without considering many important MGs and/or grid parameters. without considering many important MGs and/or grid parameters. Furthermore, the existing works in the weather conditions, future time slot power generation, energy consumption profiles, dynamic pricing, and other system factors. In this paper, an EMS is developed to reduce consumer ECC while enabling surplus energy transfer to grid and/or MGs through fuzzy-based P2P energy exchange algorithm with dynamic pricing. The novelty of the proposed EMS and the contributions of this paper are summarized as follows:

1) Modeling MG consumer load power demand, solar PV power, and wind turbine power behaviors using random vector functional link network (RVFLN) approach to predict future time slot values.
2) Developing a fuzzy-based P2P energy exchange algorithm to enable surplus energy transfer to grid and/or MGs with dynamic pricing.
3) Implementing ESS charging/discharging control and diesel generator turn ON strategy based on the MGs deficit power and consumer LPD reduction strategy based on the consumer ECC margin and energy consumption index.
4) Finally, implementing an EMS that includes both on demand supply strategy (ODSS) and consumer energy consumption cost reduction strategy (CCRS). The ODSS is a baseline strategy and the CCRS is the cost reduction strategy based on the MGs prediction models.

The rest of this paper is organized as follows. The description of the MGs and prediction models are presented in Section II. The fuzzy-based P2P energy exchange algorithm with dynamic
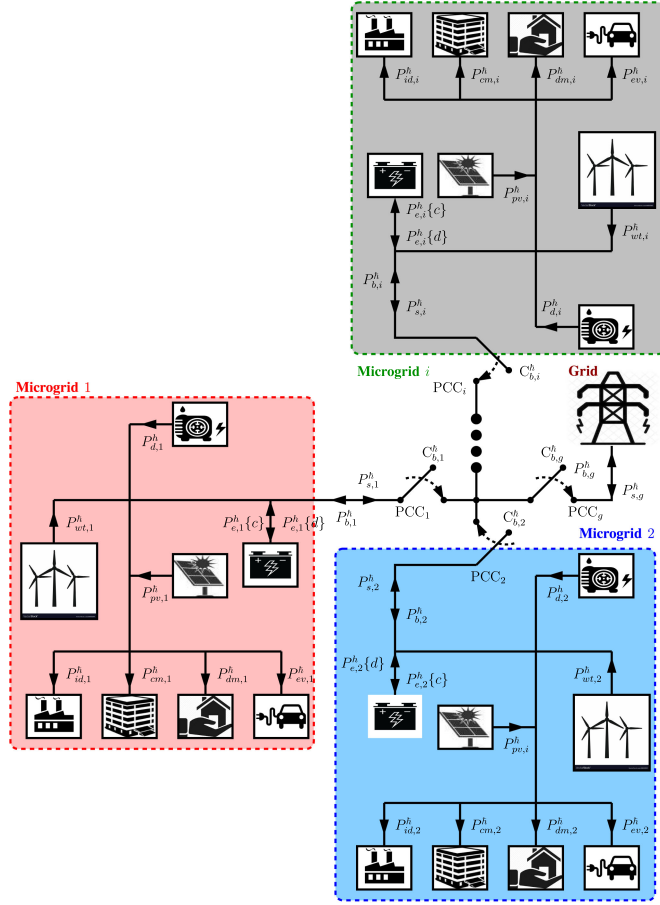
Fig. 1. Schematic representation of grid interconnected multi-microgrids.

pricing and the consumer ECC models are presented in Section III. The proposed ODSS and CCRS are presented in Section IV. Section V presents the results with the historical data followed by the conclusion in Section VI.

II. SYSTEM LEVEL MATHEMATICAL MODELING

This section presents the description of grid interconnected multi-microgrids and the system level mathematical models of MGs consumer load power demand, DGs, i.e., solar PV and wind turbine, ESSs, diesel generator, and MGs constraints. The purpose of this section is to model the grid interconnected multi-microgrids consumer LPD and energy sources. The outcomes of this section: a) future time slot values of MGs consumer LPD and DGs output power; b) ESSs energy, power, charge/discharge rate, state-of-charge (SOC), and energy cost; and c) diesel generator energy, power, and power generation cost. In addition, in this section, the MGs constraints are presented.

A. Interconnected Multi-Microgrid Model

Fig. 1 shows the schematic representation of grid interconnected multi-microgrids. Here, the number of MG is denoted as $i \in \{1, 2, 3, ..., I\}$. The ith MG consists of energy sources (i.e., solar PV, wind turbine, ESS, and diesel generator) and different types of consumer loads. Each MG is connected to

grid through the point of common coupling (PCC). Here, the MG models, i.e., DGs, ESSs, diesel generator, and consumer LPD, are developed at the system level. Also, the grid and MG circuit breakers, i.e., $C_{b,g}^{\hbar}$ and $C_{b,i}^{\hbar}$, are developed at system level. Moreover, the grid and MG circuit breakers are considered as an ON and OFF switch, i.e., $C_{b,g}^{\hbar} \in \{0, 1\}$ and $C_{b,i}^{\hbar} \in \{0, 1\}$. Thus, in this work, dynamic stability issues due to switching and synchronization are not considered. However, these issues have been extensively reported in literature and the successful control strategies can be deployed to enable the seamless integration of multi-microgrids [24], [25]. Here, $\hbar$ is defined as the sum of present ($h \in \{1, 2, ..., H-1\}$) and future (m) time slot ($\hbar = h + m$). From Fig. 1, the power balance at PCC of ith MG can be expressed as:

$$P_{ld,i}^{\hbar} + \mathcal{P}_{s,g}^{\hbar,*} + \mathcal{P}_{s,i}^{\hbar,*} = P_{dg,i}^{\hbar} + P_{e,i}^{h} + P_{d,i}^{h} + \mathcal{P}_{b,g}^{\hbar,*} + \mathcal{P}_{b,i}^{\hbar,*}. \quad (1)$$

B. System Level Models

In this section, system level mathematical models are presented according to the above-mentioned description.

1) Consumer LPD, Solar PV, and Wind Turbine Model: The stochastic nature of consumer LPD and DGs output powers are modeled using RVFLN approach, which predict future time slot values. This approach reduces iterative tuning of the weights during dataset training, ensure faster convergence, ease of computation, and less training error as compared to conventional neural network techniques [26]. In general, the dynamics and/or behaviors of MGs consumer load power demand, solar PV power, and wind turbine power are non-linear in nature with respect time [5]. Hence, deep neural network approach based on RVFLN is used in this paper as it is suitable for modeling the non-linear dynamics and/or behaviors as compared to the other linear models [26], [27]. The RVFLN transforms the inputs into a non-linear space through the use of non-linear activation functions during the predictions. The future time slot values of consumer LPD and DGs, i.e., solar PV and wind turbine, power of ith MG at time slot $\hbar$ can be expressed as:

$$P_{z,i}^{\hbar} = \sum_{j=1}^{h_l} \beta_j^z g\left(w_j^z x_{in}^z + b_j^z\right) + \sum_{j=h_l+1}^{h_l+n} \beta_j^z x_{in}^z. \quad (2)$$

In (2), the consumer LPD, solar PV power, and wind turbine power can be derived by replacing z with l, pv, and wt, respectively. Consumer LPD inputs: weekdays, weekends, month, $P_{l,i}^{m,h}$, T_{od}, H_r, and $P_{l,i}^{max}$. Solar PV inputs: $I_s^{f,h}$, A_t, $T_{pv,i}^{f,h}$, $V_w^{f,h}$, D_w, $P_{pv,i}^{f,h}$, T_{od}, H_r, and $P_{pv,i}^{r}$. Wind turbine inputs: A_p, $V_w^{f,h}$, D_w, $P_{wt,i}^{f,h}$, T_{od}, H_r, and $P_{wt,i}^{r}$. The solar PV power generation cost ($\mathbb{C}_{pv,i}^{\hbar}$) and wind turbine power generation cost ($\mathbb{C}_{wt,i}^{\hbar}$) of ith MG at time slot $\hbar$ can be calculated from [28], [29]. The mean absolute percentage error (MAPE) is used to measure the consumer LPD and DGs output power prediction error, which can be expressed as:

$$\text{MAPE}(\%) = \frac{100}{H} \sum_{h=1}^{H} \left| \left(P_{z,i}^{m,h} - P_{z,i}^{\hbar}\right) \times \left(P_{z,i}^{m,h}\right)^{-1} \right|. \quad (3)$$

2) ESS Model: Better performance of the MG can be achieved by means of ESS, which is the key technology for EMS [5]. The ESS charging energy ($E_{e,i}^h\{c\}$) and discharging energy ($E_{e,i}^h\{d\}$) of ith MG at time slot h can be expressed as:

$$E_{e,i}^h\{c\} = S_{e,i}SOC_{e,i}^h + \eta_{e,i}\int_{h_{in}}^{h_{fi}}\left(P_{sr,i}^\hbar + P_{d,i}^h + \mathcal{P}_{b,i}^{\hbar,*}\right)dh, \tag{4a}$$

$$E_{e,i}^h\{d\} = S_{e,i}SOC_{e,i}^h - \frac{1}{\eta_{e,i}}\int_{h_{in}}^{h_{fi}}\left(P_{ld,i}^\hbar - P_{dg,i}^\hbar\right)dh. \tag{4b}$$

If the ESS state-of-charge (SOC) is low, then the proposed EMS will charge the ESS with the surplus power ($P_{sr,i}^\hbar$) of ith MG at time slot $\hbar$. The ESS capacity degradation mainly depends on the SOC limits, charge rate ($C_{e,i}^h$), discharge rate ($D_{e,i}^h$), and temperature [30]. Hence, the ESS state-of-charge, $C_{e,i}^h$, and $C_{e,i}^h$ should be maintained within the limits. In this paper, a regression approach is used to estimate the ESS $C_{e,i}^h$ and $C_{e,i}^h$ of ith MG at time slot h. In addition, the ESS power can be controlled through $C_{e,i}^h$ and $D_{e,i}^h$ of ith MG at time slot h, which can be expressed as:

$$C_{e,i}^h = a_{e,i}\frac{E_{e,i}^{h,*}\{c\}}{\left(SOC_{e,i}^h \times S_{e,i} \times \Delta h \times 0.01667\right)} + b_{e,i}, \tag{5a}$$

$$D_{e,i}^h = c_{e,i}\frac{E_{e,i}^{h,*}\{d\}}{\left(SOC_{e,i}^h \times S_{e,i} \times \Delta h \times 0.01667\right)} + d_{e,i}. \tag{5b}$$

The unit of ESS discharging energies is kWh, the unit of discharge rate is 1/hour, and the unit of the MG consumer load power demand is kW. Therefore, the ESS discharge energy (kWh) should be converted into power (kW). Hence, the ESS discharging power ($P_{e,i}^h\{d\}$) is formulated. Similarly, the ESS charging power ($P_{e,i}^h\{c\}$) is formulated. The ESS charging power of ith MG at time slot h can be defined as the product of $E_{e,i}^h\{c\}$, $C_{e,i}^h$, and $\eta_{c,i}$. Similarly, the ESS discharging power of ith MG at time slot h can be calculated. To avoid the ESS over charging or discharging, the ESS state-of-charge limits are necessary for charging and discharging scenarios. Hence, the ESS state-of-charge ($SOC_{e,i}^h$) of ith MG at time slot h is formulated, which can be expressed as:

$$SOC_{e,i}^h = \begin{cases} SOC_{e,i}^{in} + \frac{\left|E_{e,i}^{h-1,*}\{c\} - E_{e,i}^{h,*}\{c\}\right|}{S_{e,i}}, & \text{if } P_{e,i}^{h,*}\{c\} < 0, \\ SOC_{e,i}^{in} - \frac{\left|E_{e,i}^{h-1,*}\{d\} - E_{e,i}^{h,*}\{d\}\right|}{S_{e,i}}, & P_{e,i}^{h,*}\{d\} \geq 0. \end{cases} \tag{6}$$

where, $E_{e,i}^{h-1,*}\{c\}$ and $E_{e,i}^{h-1,*}\{d\}$ denote the ESS charging and discharging energy reference signal of ith MG at time slot $h-1$ and $P_{e,i}^{h,*}\{c\}$, $P_{e,i}^{h,*}\{d\}$ denote the ESS charging and discharging power reference signal of ith MG at time slot h. If $P_{e,i}^{h,*}\{c\}$ is negative, then the ESS needs to charge and if $P_{e,i}^{h,*}\{d\}$ is positive, then the ESS needs to discharge. The ESS energy cost ($\mathbb{C}_{e,i}^h$) of ith MG at time slot h is calculated from [28], [29].

3) Diesel Generator Model: The diesel generator output energy ($E_{d,i}^h$) of ith MG at time slot h can be expressed as:

$$E_{d,i}^h = P_{d,i}^r \times \eta_{d,i} \times \mathcal{K}_{d,i}^{h,*} \times \mathcal{D}_{d,i}^{h,*}. \tag{7}$$

The diesel generator power generation cost ($\mathbb{C}_{d,i}^h$) of ith MG at time slot h can be expressed as:

$$\mathbb{C}_{d,i}^h = \begin{cases} \mathbb{C}_{d,i}^{in}/365 + \left(E_{d,i}^{h,*}F_{con,i}\mathbb{C}_{fc}\right), & \text{if } \mathcal{D}_{d,i}^{h,*} > 0, \\ 0, & \text{otherwise.} \end{cases} \tag{8}$$

4) MGs Constraints: Due to intermittency, the $P_{dg,i}^\hbar$ cannot meet the consumer LPD. Hence, it is necessary to identify the $P_{sr,i}^\hbar$ and deficit power ($P_{df,i}^\hbar$) of ith MG at time slot $\hbar$, which can be expressed as:

$$P_{sr,i}^\hbar = \begin{cases} 0, & \text{if } P_{dg,i}^\hbar \leq P_{ld,i}^\hbar, \\ C_{br,i}^\hbar \times \left\{P_{dg,i}^\hbar - P_{ld,i}^\hbar\right\}, & \text{otherwise.} \end{cases} \tag{9}$$

If $P_{sr,i}^\hbar$ is equal to zero, then the deficit power would be supplied from ESS or diesel generator or grid and/or MGs. The $P_{df,i}^\hbar$ of ith MG at time slot $\hbar$ can be expressed as:

$$P_{df,i}^\hbar = \begin{cases} C_{br,i}^\hbar \times \left\{P_{ld,i}^\hbar - P_{dg,i}^\hbar\right\}, & \text{if } P_{dg,i}^\hbar < P_{ld,i}^\hbar, \\ 0, & \text{otherwise.} \end{cases} \tag{10}$$

Thus, the power penetration constraint of ith MG can be expressed as:

$$\left(P_{pv,i}^\hbar + P_{wt,i}^\hbar + P_{d,i}^h + P_{e,i}^h\right) \leq P_{ld,i}^{max}. \tag{11}$$

Pirbazari *et al.* developed a house energy consumption prediction model [31]. Different types of approaches are used to predict the house energy consumption such as support vector regression approach, gradient boosting regression trees-driven approach, feedforward neural network approach, and long short-term memory network approach. The obtained mean absolute percentage error approximately ranges from 1% to 3%. Hence, in this work, 3% error has been considered for the proposed EMS for grid interconnected multi-microgrids. To improve the prediction accuracy, the below constraint is used:

$$\frac{1}{1 + \{\text{MAPE}(\%) \times 0.01\}} > 0.97. \tag{12}$$

If prediction accuracy is less than 0.97, then the strategy adjusts the RVFLN network hidden layer and network weight. Then it retrains the model and tests the model with the updated values. The ESS constraints, i.e., $SOC_{e,i}^h$, $C_{e,i}^h$, $D_{e,i}^h$, $P_{e,i}^h\{c\}$, and $P_{e,i}^h\{d\}$, are given below:

$$SOC_{e,i}^{min} \leq SOC_{e,i}^h \leq SOC_{e,i}^{max}, \tag{13a}$$

$$-C_{e,i}^{max} \leq -C_{e,i}^h \leq 0, \tag{13b}$$

$$0 \leq D_{e,i}^h \leq D_{e,i}^{max}, \tag{13c}$$

$$-P_{e,i}^{max}\{c\} \leq -P_{e,i}^h\{c\} \leq 0, \tag{13d}$$

$$0 \leq P_{e,i}^h\{d\} \leq P_{e,i}^{max}\{d\}. \tag{13e}$$

where, $SOC_{e,i}^{max}$, $SOC_{e,i}^{min}$ denote the maximum and minimum ESS state-of-charge limit of ith MG and $P_{e,i}^{max}\{c\}$, $P_{e,i}^{max}\{d\}$ denote the maximum ESS charging and discharging power limit

of ith MG. The diesel generator constraints are given below:

$$0 \leq P_{d,i}^h \leq P_{d,i}^{max} \ \& \ \sum_{h=1}^{H-1} \mathcal{D}_{d,i}^{h,*} \leq D_{d,i}^{max}. \qquad (14)$$

where, $P_{d,i}^{max}$ is the diesel generator maximum power of ith MG.

III. P2P ENERGY EXCHANGE ALGORITHM AND COST

This section presents a fuzzy-based P2P energy exchange algorithm with dynamic pricing, MGs consumer energy consumption cost, and MGs consumer ECC margin with energy consumption index. The purpose of this section is to generate the reference signal of MG consumer ECC using fuzzy-based P2P energy exchange algorithm with dynamic pricing. The outcomes of this section are reference signal of P2P energy exchange, buying/selling cost of deficit/surplus energy, total electricity consumption, consumer ECC margin, and MGs consumer energy consumption index.

A. Fuzzy-Based P2P Energy Exchange Algorithm

The fuzzy-based P2P energy exchange algorithm with dynamic pricing decides the reference signal of P2P energy exchange and the buying/selling cost of deficit/surplus energy based on the surplus energy of ith MG at time slot $\hbar$, deficit energy of ith MG at time slot $\hbar$, unique identity number of ith MG at time slot $\hbar$, and dynamic per unit electricity price. The solution steps are follows:

Step 1: Initialize the system parameter specifications and update the required information of each MG.

Step 2: The ith MG is assigned as a seller or a buyer based on the $P_{sr,i}^{\hbar}$ or $P_{df,i}^{\hbar}$. If $P_{sr,i}^{\hbar}$ is greater than zero, then the P2P energy exchange strategy sets the corresponding MG as a seller. Furthermore, if $P_{df,i}^{\hbar}$ is greater than zero, then the P2P energy exchange strategy sets the corresponding MG as a buyer. After identification of MG as a seller or a buyer, a unique identity number ($UIN_i^{\hbar}$) is assigned to each buyer and seller, which retains the unrecognizability of seller and buyer. The unique identity for buyer and seller can be expressed as:

$$UIN_i^{\hbar} = \begin{cases} 1, & \text{if } (9) > 0 \ \& \ (10) = 0, \\ 0, & \text{if } (9) \ \& \ (10) = 0, \\ -1, & \text{if } (9) = 0 \ \& \ (10) > 0. \end{cases} \qquad (15)$$

where, 1, -1, and 0 denote that the corresponding MG is a seller, buyer or is not contributing as a buyer or seller, respectively. The $UIN_i^{\hbar}$ gives the buyer and seller identities to all sellers and buyers.

Steps 3 and 4: The fuzzy logic receives the information and decide the selling and buying cost of the grid and the MG based on the $\mathcal{E}_{sr,i}^{\hbar}$, $\mathcal{E}_{df,i}^{\hbar}$, $\mathcal{E}_{p2p}^{\hbar,*}$, $UIN_i^{\hbar}$, and dynamic per unit electricity price ($\mathbb{C}_{dp}^h$). Here, the $\mathcal{E}_{sr,i}^{\hbar}$ of ith MG at time slot $\hbar$ can be defined as the product of $P_{sr,i}^{\hbar}$ of ith MG at time slot $\hbar$ and the time slot difference ($\Delta\hbar$), the $\mathcal{E}_{df,i}^{\hbar}$ of ith MG at time slot $\hbar$ can be defined as the product of $P_{df,i}^{\hbar}$ of ith MG at time slot $\hbar$ and the time slot difference, and the developed fuzzy-based P2P energy exchange algorithm with dynamic pricing decide the P2P energy exchange reference signal. The values of $\mathcal{E}_{sr,i}^{\hbar}$
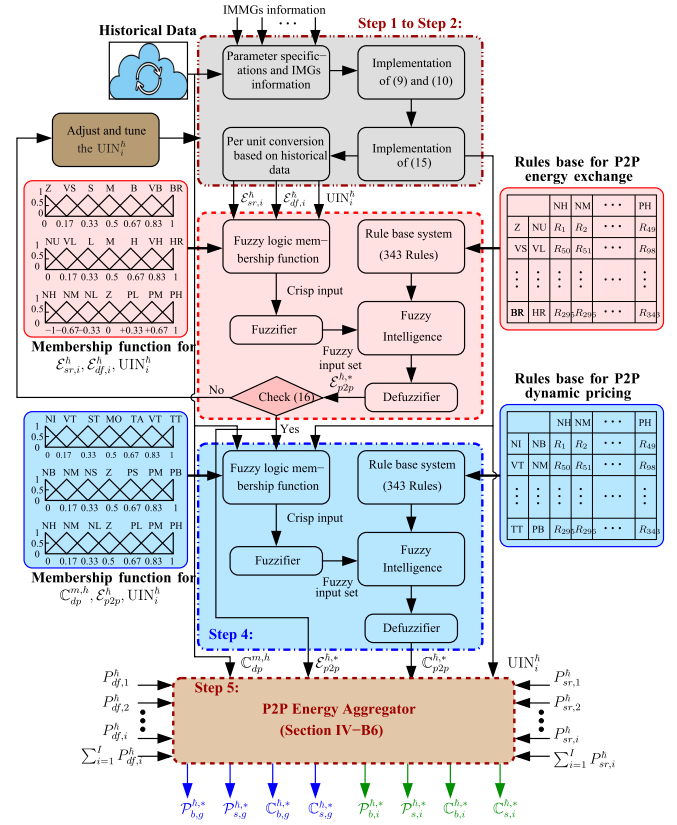

Fig. 2. Schematic representation of fuzzy-based P2P energy exchange algorithm with dynamic pricing. Here, the numbers in the brackets indicate the implementation of corresponding equation, i.e., in Step 1 to Step 2, it shows the implementation of (9) and (10), which indicate the implementation of surplus and deficit power of ith MG at time slot $\hbar$.

and $\mathcal{E}_{df,i}^{\hbar}$ of ith MG at time slot $\hbar$ depends on $P_{sr,i}^{\hbar}$ and $P_{df,i}^{\hbar}$, respectively. The value of $\mathcal{E}_{p2p}^{\hbar,*}$ depends on $\mathcal{E}_{sr,i}^{\hbar}$, $\mathcal{E}_{df,i}^{\hbar}$, and $UIN_i^{\hbar}$. To eliminate the complex mathematical model and/or control strategy, the fuzzy logic is the most appropriate control logic for handling multiple information [32]. Hence, in this paper, the fuzzy logic strategy is considered, which decides the reference signal of P2P surplus energy exchange and buying/selling cost of deficit/surplus energy by modeling the MG information with simple IF-THEN rules. Here, the center of gravity method is used for defuzzification and Mamdani type inference engine is used for the implication of fuzzy logic rule base. Moreover, triangular membership function is used for both fuzzy logic input and output, which is shown in Fig. 2. A total of 686 rules, i.e., 343 rules in Step 3 and 343 rules in Step 4, are developed and hence the fuzzy logic rules are not shown. In Step 3, seven fuzzy subsets are chosen for the inputs, i.e., $\mathcal{E}_{sr,i}^{\hbar}$, $\mathcal{E}_{df,i}^{\hbar}$, $UIN_i^{\hbar}$, and output, i.e., $\mathcal{E}_{p2p}^{\hbar,*}$. Fuzzy subsets for $\mathcal{E}_{sr,i}^{\hbar}$: zero (Z), very small (VS), small (S), medium (M), big (B), very big (VB), and bigger (BR); fuzzy subsets for $\mathcal{E}_{df,i}^{\hbar}$: Null (NU), very low (VL), low (L), neutral (N), high (H), very high (VH), and higher (HR); and fuzzy subsets for $UIN_i^{\hbar}$: negative high (NH), negative medium (NM), negative low (NL), zero (Z), positive low (PL), positive medium (PM), and positive high (PH). In Step 4, seven

fuzzy subsets are chosen for the inputs, i.e., $\mathbb{C}_{dp}^{h}$, $\mathcal{E}_{p2p}^{\hbar,*}$, $\text{UIN}_{i}^{\hbar}$, and output, i.e., $\mathbb{C}_{p2p}^{\hbar,*}$. Fuzzy subsets for $\mathbb{C}_{dp}^{h}$: Nil (NI), very short (VT), short (ST), moderate (MO), tall (TA), very tall (VT), and tallest (TT); and fuzzy subsets for $\mathcal{E}_{p2p}^{\hbar,*}$: negative big (NB), negative medium (NM), negative small (NS), zero (Z), positive small (PS), positive medium (PM), and positive big (PB). The strategy decides $\mathcal{E}_{p2p}^{\hbar,*}$ based on the $\mathcal{E}_{sr,i}^{\hbar}$, $\mathcal{E}_{df,i}^{\hbar}$, and $\text{UIN}_{i}^{\hbar}$ in Step 3. In addition, it decides $\mathbb{C}_{p2p}^{\hbar,*}$ based on the $\mathbb{C}_{dp}^{h}$, $\mathcal{E}_{p2p}^{\hbar,*}$ and $\text{UIN}_{i}^{\hbar}$ in Step 4. The net energy exchange to grid and/or i^{th} MG must satisfy the below condition:

$$\pm\mathcal{E}_{p2p}^{\hbar,*} \leq I^{-1} \sum_{i=1}^{I} \left(P_{sr,i}^{max} + P_{df,i}^{max} \right) \Delta h. \tag{16}$$

where, $P_{sr,i}^{max}$ and $P_{df,i}^{max}$ denote the maximum surplus and deficit power of ith MG at time slot $\hbar$.

Step 5: The P2P energy exchange aggregator receives information of $\mathcal{E}_{p2p}^{\hbar,*}$, $\mathbb{C}_{p2p}^{\hbar,*}$, $\mathbb{C}_{dp}^{h}$, $P_{df,i}^{\hbar}$, and $P_{sr,i}^{\hbar}$. Then, it allocates the reference signal to grid and/or MGs, which is described in Section IV-B7.

B. Consumer ECC Model

The total electricity consumption $(\mathcal{E}_{con,i}^{\hbar})$ of ith MG at time slot $\hbar$ can be defined as the sum of ith MG consumer load power demand, i^{th} MG power losses, and ESS charging power, which can be expressed as:

$$\mathcal{E}_{con,i}^{\hbar} = \left(P_{l,i}^{\hbar} + P_{loss,i}^{\hbar} + \left| P_{e,i}^{\hbar}\{c\} \right| \right) \times \Delta h. \tag{17}$$

The total ECC $(\mathbb{E}_{cost,i}^{\hbar})$ of ith MG at time slot $\hbar$ can be defined as the function of total electricity consumption of ith MG at time slot $\hbar$, electricity price $(\mathbb{C}_{i}^{\hbar})$ of ith MG at time slot $\hbar$, selling cost $(\mathbb{S}_{cost,i}^{\hbar})$ of ith MG at time slot $\hbar$, and buying cost $(\mathbb{B}_{cost,i}^{\hbar})$ of ith MG at time slot $\hbar$. The $\mathbb{E}_{cost,i}^{\hbar}$ of ith MG at time slot $\hbar$ can be expressed as:

$$\mathbb{E}_{cost,i}^{\hbar} = \left(\mathbb{C}_{i}^{\hbar} \times \mathcal{E}_{con,i}^{\hbar} - \left\{ \mathbb{S}_{cost,i}^{\hbar} - \mathbb{B}_{cost,i}^{\hbar} \right\} \right). \tag{18}$$

If $P_{dg,i}^{\hbar} > 0$, then the $\mathbb{C}_{i}^{\hbar}$ can be calculated from (19). Otherwise, $\mathbb{C}_{i}^{\hbar}$ is equal to $\mathbb{C}_{dp}^{h}$.

$$\mathbb{C}_{i}^{\hbar} = \begin{cases} \frac{\mathbb{C}_{pv,i}^{\hbar} + \mathbb{C}_{wt,i}^{\hbar}}{\mathcal{E}_{con,i}^{\hbar}}, & \text{if } P_{sr,i}^{\hbar} < 0, \\ \frac{\mathbb{C}_{pv,i}^{\hbar} + \mathbb{C}_{wt,i}^{\hbar} + \mathbb{C}_{e,i}^{\hbar} + \mathbb{C}_{d,i}^{\hbar} \pm \mathbb{C}_{p2p}^{\hbar,*}}{\mathcal{E}_{con,i}^{\hbar}}, & \text{if } P_{sr,i}^{\hbar} = 0, \\ \frac{\mathbb{C}_{pv,i}^{\hbar} + \mathbb{C}_{wt,i}^{\hbar} + \mathbb{C}_{e,i}^{\hbar} + \mathbb{C}_{d,i}^{\hbar} \pm \mathbb{C}_{p2p,i}^{\hbar,*} \pm \mathbb{C}_{p2p,g}^{\hbar,*}}{\mathcal{E}_{con,i}^{\hbar}}, & \text{otherwise.} \end{cases} \tag{19}$$

The $\mathbb{S}_{cost,i}^{\hbar}$ and $\mathbb{B}_{cost,i}^{\hbar}$ of ith MG at time slot $\hbar$ can be expressed as:

$$\mathbb{S}_{cost,i}^{\hbar} = \left\{ \left(\mathbb{C}_{s,i}^{\hbar,*} \mathcal{P}_{s,i}^{\hbar,*} \right) + \left(\mathbb{C}_{s,g}^{\hbar,*} \mathcal{P}_{s,g}^{\hbar,*} \right) \right\} \Delta h,$$

$$\mathbb{B}_{cost,i}^{\hbar} = \left\{ \left| \mathbb{C}_{b,i}^{\hbar,*} \mathcal{P}_{b,i}^{\hbar,*} \right| + \left| \mathbb{C}_{b,g}^{\hbar,*} \mathcal{P}_{b,g}^{\hbar,*} \right| \right\} \Delta h. \tag{20}$$

C. Consumer ECC Margin and Energy Consumption Index

The consumer ECC margin $(\text{M}_{ecc,i}^{\hbar})$ of ith MG at time slot $\hbar$ is hard to estimate. The regression approach has been developed

to predict and/or estimate the supermarket, building, and residential unit energy consumption [33]–[35]. Hence, in this paper, a regression approach is used to estimate the consumer energy consumption index $(\text{I}_{ec,i}^{\hbar})$ of ith MG at time slot $\hbar$. In (21), the total energy consumption of ith MG at time slot $\hbar$ is converted into per unit value, i.e., $\mathcal{E}_{con,i}^{\hbar} \times \mathcal{E}_{con,i}^{max^{-1}}$. Also, the $\text{M}_{ecc,i}^{\hbar}$ is decided based on the $\text{I}_{ec,i}^{\hbar}$, which can be expressed as:

$$\text{I}_{ec,i}^{\hbar} = \left(a_i e^{-b_i \mathcal{R}_i^{\hbar}} + c_i \right) \times \frac{\mathcal{E}_{con,i}^{\hbar}}{\mathcal{E}_{con,i}^{max}}. \tag{21}$$

The reliability of the network or energy index of reliability has been developed in [28]. In this paper, the reliability index $(\mathcal{R}_i^{\hbar})$ of ith MG at time slot $\hbar$ is formulated based on the [28]. The $\mathcal{R}_i^{\hbar}$ of ith MG at time slot $\hbar$ can be defined as the ratio of difference in the consumer load power demand of ith MG at time slot $\hbar$ and power supplied from the ith MG energy sources at time slot $\hbar$ and the consumer load power demand of ith MG at time slot $\hbar$, which is given in (22). Here, $\mathcal{R}_i^{\hbar} < 1$ denotes the expected power not supplied to the ith MG at time slot $\hbar$ and $\mathcal{R}_i^{\hbar} = 1$ denotes the expected power supplied to the ith MG at time slot $\hbar$. In this paper, threshold limits are considered for the reliability index, i.e., maximum and minimum threshold limits. The proposed EMS maintains the reliability index of ith MG at time slot $\hbar$ within the threshold limits. The $\mathcal{R}_i^{\hbar}$ of ith MG at time slot $\hbar$ can be expressed as:

$$\mathcal{R}_i^{\hbar} = 1 - \frac{\left\{ P_{dg,i}^{\hbar} + P_{e,i}^{\hbar} + P_{d,i}^{\hbar} \pm \mathcal{P}_{p2p,i}^{\hbar,*} \pm \mathcal{P}_{p2p,g}^{\hbar,*} \right\}}{P_{ld,i}^{\hbar}}. \tag{22}$$

Set of rules are developed to decide $\text{M}_{ecc,i}^{\hbar}$ of ith MG at time slot $\hbar$. The rules are defined as IF-THEN structure and its formulated based on the (10), (18), (21), and (22).

1) If $0.97 \leq \mathcal{R}_i^{\hbar} \leq 1$ & $\text{I}_{ec,i}^{\hbar} \leq \text{I}_{ec,i}^{min}$ & $\mathbb{E}_{cost,i}^{\hbar} \leq \mathbb{E}_{cost,i}^{min,\hbar}$ & $P_{df,i}^{\hbar} = 0$, then $\text{M}_{ecc,i}^{\hbar}$ = very small (VS).

2) If $0.97 \leq \mathcal{R}_i^{\hbar} \leq 1$ & $\text{I}_{ec,i}^{min} < \text{I}_{ec,i}^{\hbar} < (\text{I}_{ec,i}^{min} + \frac{\Delta \text{I}_{ec,i}^{\hbar}}{4})$ & $\mathbb{E}_{cost,i}^{min,\hbar} < \mathbb{E}_{cost,i}^{\hbar} < (\mathbb{E}_{cost,i}^{min,\hbar} + \frac{\Delta \mathbb{E}_{cost,i}^{\hbar}}{4})$ & $P_{df,i}^{min} < P_{df,i}^{\hbar} < (P_{df,i}^{min} + \frac{\Delta P_{df,i}^{\hbar}}{4})$, then $\text{M}_{ecc,i}^{\hbar}$ = small (S).

3) If $0.97 \leq \mathcal{R}_i^{\hbar} \leq 1$ & $(\text{I}_{ec,i}^{min} + \frac{\Delta \text{I}_{ec,i}^{\hbar}}{4}) < \text{I}_{ec,i}^{\hbar} < (\text{I}_{ec,i}^{min} + \frac{\Delta \text{I}_{ec,i}^{\hbar}}{2})$ & $(\mathbb{E}_{cost,i}^{min,\hbar} + \frac{\Delta \mathbb{E}_{cost,i}^{\hbar}}{4}) < \mathbb{E}_{cost,i}^{\hbar} < (\mathbb{E}_{cost,i}^{min,\hbar} + \frac{\Delta \mathbb{E}_{cost,i}^{\hbar}}{2})$ & $(P_{df,i}^{min} + \frac{\Delta P_{df,i}^{\hbar}}{4}) < P_{df,i}^{\hbar} < (P_{df,i}^{min} + \frac{\Delta P_{df,i}^{\hbar}}{2})$, then $\text{M}_{ecc,i}^{\hbar}$ = low (L).

4) If $0.97 \leq \mathcal{R}_i^{\hbar} \leq 1$ & $\text{I}_{ec,i}^{\hbar} = (\text{I}_{ec,i}^{min} + \frac{\Delta \text{I}_{ec,i}^{\hbar}}{2})$ & $\mathbb{E}_{cost,i}^{\hbar} = (\mathbb{E}_{cost,i}^{min,\hbar} + \frac{\Delta \mathbb{E}_{cost,i}^{\hbar}}{2})$ & $P_{df,i}^{\hbar} = (P_{df,i}^{min} + \frac{\Delta P_{df,i}^{\hbar}}{2})$, then $\text{M}_{ecc,i}^{\hbar}$ = medium (M).

5) If $0.97 \leq \mathcal{R}_i^{\hbar} \leq 1$ & $(\text{I}_{ec,i}^{min} + \frac{\Delta \text{I}_{ec,i}^{\hbar}}{2}) < \text{I}_{ec,i}^{\hbar} < (\text{I}_{ec,i}^{min} + \frac{3\Delta \text{I}_{ec,i}^{\hbar}}{4})$ & $(\mathbb{E}_{cost,i}^{min,\hbar} + \frac{\Delta \mathbb{E}_{cost,i}^{\hbar}}{2}) < \mathbb{E}_{cost,i}^{\hbar} < (\mathbb{E}_{cost,i}^{min,\hbar} + \frac{3\Delta \mathbb{E}_{cost,i}^{\hbar}}{4})$ & $(P_{df,i}^{min} + \frac{\Delta P_{df,i}^{\hbar}}{2}) < P_{df,i}^{\hbar} < (P_{df,i}^{min} + \frac{3\Delta P_{df,i}^{\hbar}}{4})$, then $\text{M}_{ecc,i}^{\hbar}$ = high (H).

6) If $0.97 \leq \mathcal{R}_i^{\hbar} \leq 1$ & $(\text{I}_{ec,i}^{min} + \frac{3\Delta \text{I}_{ec,i}^{\hbar}}{4}) < \text{I}_{ec,i}^{\hbar} < (\text{I}_{ec,i}^{min} + \Delta \text{I}_{ec,i}^{\hbar})$ & $(\mathbb{E}_{cost,i}^{min,\hbar} + \frac{3\Delta \mathbb{E}_{cost,i}^{\hbar}}{4}) < \mathbb{E}_{cost,i}^{\hbar} <$

$(\mathbb{E}^{min,\hbar}_{cost,i} + \Delta\mathbb{E}^{\hbar}_{cost,i})$ & $(P^{min}_{df,i} + \frac{3\Delta P^{\hbar}_{df,i}}{4}) < P^{\hbar}_{df,i} < (P^{min}_{df,i} + \Delta P^{\hbar}_{df,i})$, then $M^{\hbar}_{ecc,i} = $ big (B).

7) If $0.97 \leq \mathcal{R}^{\hbar}_i \leq 1$ & $I^{\hbar}_{ec,i} > (I^{min}_{ec,i} + \Delta I^{\hbar}_{ec,i})$ & $\mathbb{E}^{\hbar}_{cost,i} > \mathbb{E}^{max,\hbar}_{cost,i}$ & $P^{\hbar}_{df,i} > (P^{min}_{df,i} + \Delta P^{\hbar}_{df,i})$, then $M^{\hbar}_{ecc,i} = $ very big (VB).

The next section presents the proposed EMS for grid interconnected MGs to achieve the ECC reduction based on the predicted values and MGs information. The developed EMS includes ODSS and CCRS. The ODSS is the baseline strategy, which aims to sell/buy the surplus/deficit energy to/from grid. The CCRS is the MGs consumer ECC reduction strategy using fuzzy-based P2P energy exchange algorithm with dynamic pricing. The outcomes of this section are MGs consumer ECC, total electricity consumption, consumer ECC margin, and MGs consumer energy consumption index for ODSS and CCRS approach.

IV. PROPOSED ENERGY MANAGEMENT STRATEGY

The main objective is to reduce the multi-microgrid (MG) consumer energy consumption cost (ECC) using fuzzy-based peer-to-peer (P2P) energy exchange algorithm with dynamic pricing. Here, the cost reduction problem can be expressed in terms of MG power balance equation and MG consumer ECC, which are given in (1) and (18), respectively. These equations clearly show that the objective is to increase surplus energy exchange to grid and/or MGs, decrease deficit energy buying from grid, utilize ESS energy, and decrease diesel generator operating hours. To solve the consumer ECC reduction problem, two strategies, i.e., on demand supply strategy and consumer energy consumption cost reduction strategy, are proposed. The strategies rely on the MG power generation/demand prediction models, MG information, and historical data.

A. On Demand Supply Strategy

The ODSS is the baseline strategy, which aims to sell/buy the surplus/deficit energy to/from grid. The ODSS provides better energy consumption cost saving by considering the surplus energy selling to grid or turn ON diesel generator with respect to cost. The ODSS problem ($\mathcal{J}_1$) can be formulated with respect to reference signals such as $E^{\hbar,*}_{e,i}$ and $E^{\hbar,*}_{d,i}$ at time slot h, which can be expressed as:

$$\mathcal{J}_1 = \min_{\left[E^{\hbar,*}_{e,i}, E^{\hbar,*}_{d,i}\right]} \sum_{h=1}^{H-1} \left(\alpha \frac{\mathbb{E}^{\hbar}_{cost,i}\left[E^{\hbar,*}_{e,i}, E^{\hbar,*}_{d,i}\right]}{\mathbb{E}^{max}_{cost,i}} + \{1-\alpha\} \frac{M^{h}_{ecc,i}}{M^{max}_{ecc,i}} \right)$$

s.t. Models :$(2)-(10), (17)-(20), \forall\hbar$

Constraints:$(1), (11), (12), (13a), (14), \forall\hbar$

Reliability index :$\mathcal{R}^{\hbar}_i = 1, \forall\hbar$

Cost limits :$\mathcal{S}^{\hbar}_{cost,i}$ & $\mathcal{B}^{\hbar}_{cost,i} \in \{0, 1, 2, ..., \infty\}, \forall\hbar$

P2P limits :$\mathcal{E}^{\hbar,*}_{p2p,i} = 0, C^{\hbar}_{br,g} \in \{0, 1\}, \forall\hbar.$ (23)

Here, α is the objective balancing variable, i.e., $0 \leq \alpha \leq 1$. Fig. 3 shows the functional flow chart of ODSS approach, which is divided into five modes such as surplus mode (SM), storing
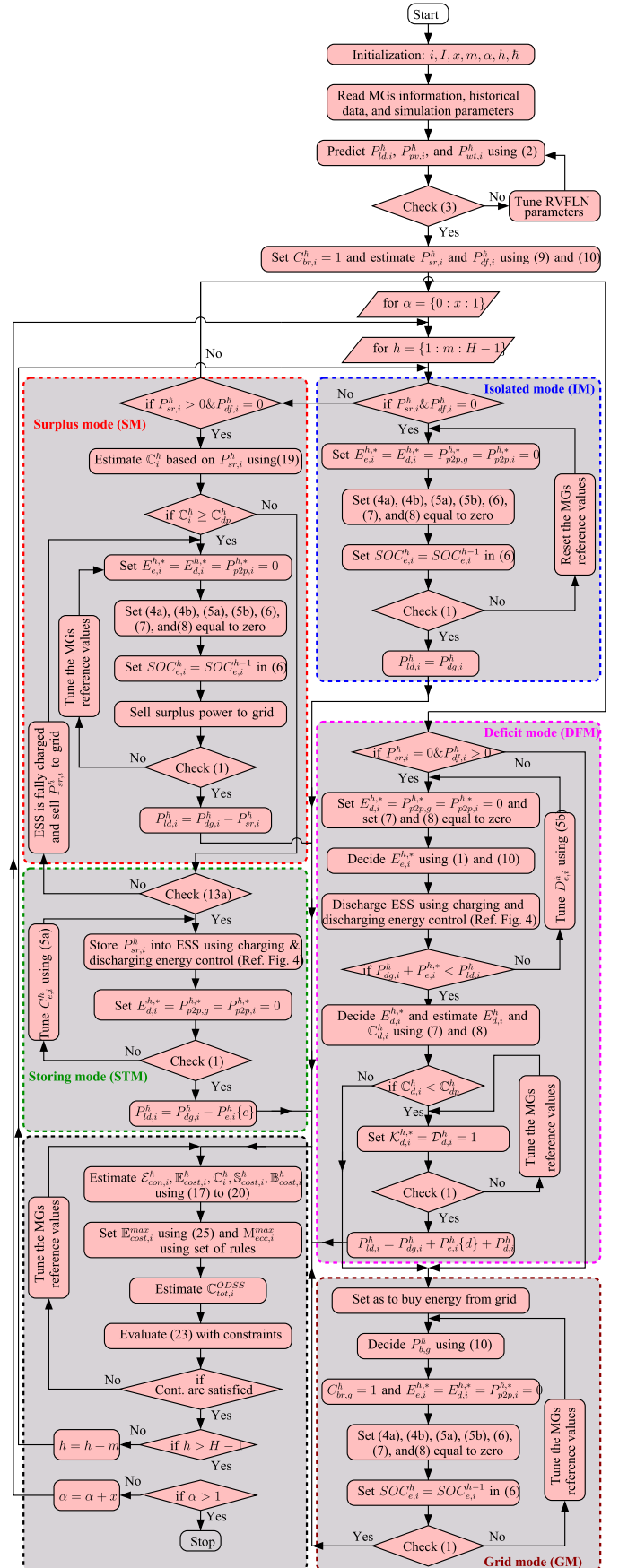

Fig. 3. Functional flowchart of on demand supply strategy (ODSS).

mode (STM), deficit mode (DFM), isolated mode (IM), and grid mode (GM). In SM, the surplus energy of ith MG is sold to the grid based on the cost. In STM, the surplus energy would be stored into the ESS while selling cost is less than the generation cost and the ESS state-of-charge is less than the maximum value. In DFM, if (10) is greater than zero, then the ODSS decides to buy energy from grid or turn ON diesel generator to supply the deficit energy. In IM, the corresponding MG is disconnected from the grid, when (9) is greater than zero and (10) is equal to zero. In GM, the ODSS decides to buy the deficit energy from grid. Satisfied

B. Consumer Energy Consumption Cost Reduction Strategy

The ODSS supplies the required LPD to consumer or buys the deficit power from grid while the demand exceeds generation or sell surplus power to grid while generation exceeds demand. However, the base line strategy is challenged, if generation exceeds the demand during off-peak hours and energy storage system SOC level is less than maximum limits, then the strategy does not need to sell energy to grid. It can be stored into the ESS and sell or use during peak hours. If MGs upcoming information is available/predicted, then the strategy provides better ECC savings for MG consumer. The proposed CCRS decides $\mathcal{E}_{p2p,i}^{\hbar,*}$, $\mathcal{E}_{p2p,g}^{\hbar,*}$, $\mathbb{C}_{p2p,i}^{\hbar,*}$, and $\mathbb{C}_{p2p,g}^{\hbar,*}$ using fuzzy-based P2P energy exchange algorithm with dynamic pricing, upcoming information of MGs, and historical data. The upcoming information of MGs, and historical data. The consumer ECC reduction problem ($\mathcal{J}_2$) can be expressed as:

$$\mathcal{J}_2 = \min_{\left[\mathcal{E}_{p2p}^{\hbar,*}, E_{e,i}^{h,*}, E_{d,i}^{h,*}\right]} \sum_{h=1}^{H-1} \left(\alpha \frac{\mathbb{E}_{cost,i}^{\hbar}\left[\mathcal{E}_{p2p}^{\hbar,*}, E_{e,i}^{h,*}, E_{d,i}^{h,*}\right]}{\mathbb{E}_{cost,i}^{max}} \right.$$
$$\left. + \{1-\alpha\} \frac{\mathrm{M}_{ecc,i}^{h}}{\mathrm{M}_{ecc,i}^{max}} \right)$$

s.t. Models :$(2)-(10),(15),(17)-(22), \forall \hbar$

Constraints :$(1),(11)-(14),(16), \forall \hbar$

Reliability index :$\mathcal{R}_i^{min} \leq \mathcal{R}_i^{\hbar} \leq \mathcal{R}_i^{max}, \forall \hbar$

Energy index :$\mathrm{I}_{ec,i}^{min} \leq \mathrm{I}_{ec,i}^{\hbar} \leq \mathrm{I}_{ec,i}^{max}, \forall \hbar$

Cost margin :$\mathrm{L} \leq \mathrm{M}_{ecc,i}^{h} \leq \mathrm{VB}, \forall \hbar$

Cost limit : $\begin{array}{c} 0 \leq \mathbb{S}_{cost,i}^{\hbar} \leq \mathbb{S}_{cost,i}^{max} \\ -\mathbb{B}_{cost,i}^{max} \leq -\mathbb{B}_{cost,i}^{\hbar} \leq 0 \end{array}, \forall \hbar$

P2P limit :$0 \leq \pm\mathcal{E}_{p2p}^{\hbar,*} \leq \pm\mathcal{E}_{p2p}^{max}, \forall \hbar$

$\mathrm{C}_{br,i}^{\hbar} \in \{0,1\}, \mathrm{C}_{br,g}^{\hbar} \in \{0,1\}, \forall \hbar. \qquad (24)$

The proposed CCRS aims to reduce $\mathbb{E}_{cost,i}^{\hbar}$, maintaining the MG consumer ECC margin within the threshold limits, i.e., $\mathrm{VS} \leq \mathrm{M}_{ecc,i}^{\hbar} \leq \mathrm{M}$, and maintaining the reliability index within the limits, i.e., $0.97 \leq \mathcal{R}_i^h \leq 1$. It is observed from (24), that the consumer ECC of each MG at time slot $\hbar$ may increase/decrease

by deciding $\mathcal{E}_{p2p,i}^{\hbar,*}$, $\mathcal{E}_{p2p,g}^{\hbar,*}$, $\mathbb{C}_{p2p,i}^{\hbar,*}$, and $\mathbb{C}_{p2p,g}^{\hbar,*}$. The characteristics of the objective function or optimization model, i.e., $\mathcal{J}_1$ and $\mathcal{J}_2$, depends on the objective balancing variable, i.e., $0 \leq \alpha \leq 1$. Lower values, i.e., $0 \leq \alpha < 0.5$, for the objective balancing variable denote the lower consumer energy consumption cost reduction and higher consumer ECC margin while higher values, i.e., $0.5 < \alpha \leq 1$, denote the higher consumer energy consumption cost reduction and lower consumer ECC margin. In this paper, the ODSS and CCRS approach objective functions are given in (23), and (24), respectively. The developed models, i.e., consumer LPD and DGs output power, are non-linear and hence, the proposed problem formulation is a non-linear programming problem. The detailed solution steps are given below:

1) Data Preprocessing and Preparation for Simulation Study: The historical raw data collected from typical MGs and weather condition data may contain lost and/or missing data points. Due to missing data points, the prediction models give inaccurate results. Hence, the collected historical raw data to be preprocessed to improve prediction accuracy. Here, the missing data points in the historical raw data is cleaned and replaced by data imputation.

2) Consumer LPD and DGs Power Prediction Using RVFLN Approach: The proposed CCRS predicts the ith MG consumer LPD and DGs power using RVFLN approach for the future time slot. Then, it estimates MAPE using (3) and checks the error limit constraints using (12). If (12) is satisfied, then the proposed CCRS uses the predicted values. Otherwise, the proposed CCRS tunes the network parameters to reduce the error between predicted and measured values.

3) Estimation of Surplus and Deficit Power: The proposed CCRS estimates the surplus and deficit power based on the prediction model results by using (9) and (10), respectively. If (9) is greater than zero and (10) is equal to zero, then the CCRS decides to estimate the $\mathcal{E}_{p2p}^{\hbar,*}$ and $\mathbb{C}_{p2p}^{\hbar,*}$. If (9) is equal to zero and (10) is greater than zero, then the CCRS decides to utilize ESS and/or diesel generator energy. Otherwise, the proposed CCRS decides to buy energy from grid and/or MGs based on the dynamic pricing.

4) Threshold Limits for Consumer ECC: The threshold limits play a major role to reduce the consumer ECC based on the dynamic pricing of DGs energy selling/buying cost. The minimum ($\mathbb{E}_{cost,i}^{min,\hbar}$) and maximum ($\mathbb{E}_{cost,i}^{max,\hbar}$) threshold limits for consumer ECC of ith MG at time slot $\hbar$ can be expressed as:

$$\mathbb{E}_{cost,i}^{min,\hbar} = \min \left(\frac{1}{n} \sum_{k=1}^{n} \mathbb{E}_{cost,i}^{h-k}, \mathbb{E}_{cost,i}^{\hbar}, \left|\mathbb{S}_{cost,i}^{\hbar}\right|, \right.$$
$$\left. \mathbb{B}_{cost,i}^{\hbar}, \mathbb{C}_{dp}^{h} \right).$$

$$\mathbb{E}_{cost,i}^{max,\hbar} = \max \left(\frac{1}{n} \sum_{k=1}^{n} \mathbb{E}_{cost,i}^{h-k}, \mathbb{E}_{cost,i}^{\hbar}, \left|\mathbb{S}_{cost,i}^{\hbar}\right|, \right.$$
$$\left. \mathbb{B}_{cost,i}^{\hbar}, \mathbb{C}_{dp}^{h} \right). \qquad (25)$$

5) Estimation of ECC Margin: The proposed CCRS estimates the MGs consumer $\mathrm{I}_{ec,i}^{\hbar}$ and $\mathcal{R}_i^{\hbar}$ using (21) and (22),
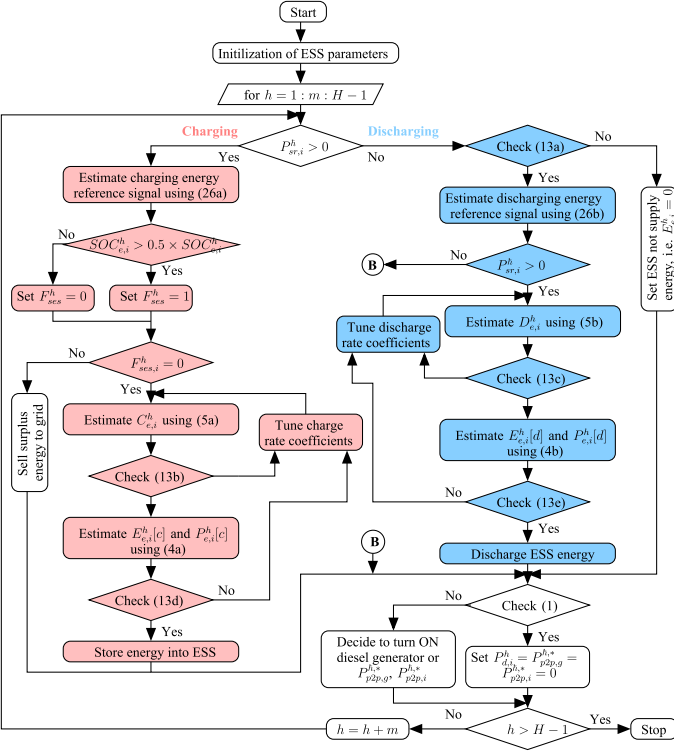
Fig. 4. Functional flowchart for energy storage systems charging and discharging energy control.

respectively. Then the MGs consumer ECC margin is estimated using the set of rules developed in Section III-C.

6) ESS Charging/Discharging Energy Control: The ESS lifetime depends on the charge/discharge rate, SOC limits, and operating temperature [5]. Therefore, a control strategy is essential to control the ESS charge/discharge rate with proper SOC limits, which is illustrated in Fig. 4. The ESS reference signal of ith MG at time slot h can be expressed as:

$$\left| E_{e,i}^{h,*} \{c\} \right| \times C_{e,i}^h = \begin{cases} P_{sr,i}^{\hbar}, & \text{if } P_{sr,i}^{\hbar} > 0 \,\&\, \mathcal{D}_{d,i}^{h,*} = 0, \\ P_{d,i}^h, & \text{if } P_{sr,i}^{\hbar} = 0 || \mathcal{D}_{d,i}^{h,*} > 0, \\ 0, & \text{otherwise.} \end{cases} \tag{26a}$$

$$E_{e,i}^{h,*} \{d\} \times D_{e,i}^h = \begin{cases} P_{df,i}^{\hbar}, & \text{if } (13a), \\ 0, & \text{otherwise.} \end{cases} \tag{26b}$$

7) Decide P2P Energy Exchange to Grid and/or MGs: The fuzzy-based P2P energy exchange algorithm decides $\mathcal{E}_{p2p}^{\hbar,*}$ and $\mathbb{C}_{p2p}^{\hbar,*}$, which can be distributed among the grid and/or MGs through P2P energy exchange aggregator. If $\mathcal{E}_{p2p}^{\hbar,*} \geq 0$, then it estimates $\mathcal{P}_{s,i}^{\hbar,*}$ and $\mathbb{C}_{s,i}^{\hbar,*}$. Otherwise, it estimates $\mathcal{P}_{b,i}^{\hbar,*}$ and $\mathbb{C}_{b,i}^{\hbar,*}$, which can be expressed as:

$$\mathcal{P}_{s,i}^{\hbar,*} = \frac{P_{sr,i}^{\hbar} \times \text{UIN}_i^{\hbar} \times \mathcal{E}_{p2p}^{\hbar,*}}{\sum_{i=1}^I P_{sr,i}^{\hbar} \times \Delta h}; \mathbb{C}_{s,i}^{\hbar,*} = \frac{1}{I} \times \mathcal{P}_{s,i}^{\hbar,*} \times \Delta h \times \mathbb{C}_{p2p}^{\hbar,*}. \tag{27}$$

$$\mathcal{P}_{b,i}^{\hbar,*} = \frac{P_{df,i}^{\hbar} \times \text{UIN}_i^{\hbar} \times \mathcal{E}_{p2p}^{\hbar,*}}{\sum_{i=1}^I P_{df,i}^{\hbar} \times \Delta h}; \mathbb{C}_{b,i}^{\hbar,*} = \frac{1}{I} \times \mathcal{P}_{b,i}^{\hbar,*} \times \Delta h \times \mathbb{C}_{p2p}^{\hbar,*}. \tag{28}$$

Similarly, the P2P energy exchange aggregator estimates the reference signal for grid selling power and buying power.

8) Consumer LPD Reduction Strategy: The consumer LPD of ith MG at time slot $\hbar$ is reduced based on the $\text{M}_{ecc,i}^h$ and $\mathcal{R}_i^{\hbar}$. Here, the objective is to generate consumer LPD reference signal $(P_{ld,i}^{\hbar,*})$ and maintain the $\mathcal{R}_i^h$ and $\text{M}_{ecc,i}$ within the threshold limits of ith MG at time slot $\hbar$. The reference signal of reduced consumer LPD is given below:

$$P_{ld,i}^{\hbar,*} = \begin{cases} P_{ld,i}^{\hbar} \mathcal{R}_i^{\hbar}, & \text{if } \begin{array}{l} \mathcal{R}_i^{min} \leq \mathcal{R}_i^{\hbar} \leq \mathcal{R}_i^{max}, \\ \text{L} \leq \text{M}_{ecc,i}^h \leq \text{H}, \end{array} \\ P_{ld,i}^{\hbar}, & \text{otherwise.} \end{cases} \tag{29}$$

9) Decide Diesel Generator Turned ON Duration: The diesel generator reference power signal of ith MG at time slot h can be expressed as:

$$E_{d,i}^{h,*} \times \left(\Delta \mathcal{D}_{d,i}^{h,*} \right)^{-1} = \left(P_{ld,i}^{\hbar} \pm P_{p2p,i}^{\hbar,*} \right) - \left(P_{dg,i}^{\hbar} + P_{e,i}^{h,*} \right). \tag{30}$$

If $E_{d,i}^{h,*}$ is less than or equal to zero, then set $D_{d,i}^{h,*} = \mathcal{K}_{d,i}^{h,*} = 0$. Else, the $\mathcal{K}_{d,i}^{h,*}$ and $\mathcal{D}_{d,i}^{h,*}$ are decided based on the $P_{df,i}^{\hbar}$ and $\mathcal{E}_{p2p}^{\hbar,*}$, which can be expressed as:

$$\mathcal{K}_{d,i}^{h,*} = \frac{\left(P_{ld,i}^{\hbar,*} + \frac{E_{e,i}^{h,*}\{c\}}{\Delta h} \right) - \left(P_{dg,i}^{\hbar} + P_{e,i}^{h,*}\{d\} + P_{b,i}^{\hbar} \right)}{\eta_{d,i} P_{d,i}^r}. \tag{31a}$$

$$\mathcal{D}_{d,i}^{h,*} = \frac{\left[\left(SOC_{e,i}^{max} - SOC_{e,i}^h \right) S_{e,i} + P_{d,i}^{h,*} \Delta h \right]}{\eta_{d,i} P_{d,i}^r}. \tag{31b}$$

10) Evaluation of Objective Function With Error Tolerance: The (24) is evaluated by varying α with constraints. Here, $\alpha = 0.25$ denote that the proposed CCRS give less preference for MG consumer energy consumption cost reduction and higher preference for MG consumer ECC margin. The MGs consumer ECC reduction problem might still be infeasible because sometimes, the specific constraints, i.e., $\text{I}_{ec,i}^{\hbar}$, could not be satisfied using proposed CCRS based on the predicted values and historical information. Therefore, we adjust the unsatisfied constraints in order to overcome such problem, for example, we relax the constraint, if not be satisfied at time slot $\hbar$. Here, the $\text{I}_{ec,i}^{\hbar}$ is modified with an error tolerance, which can be expressed as:

$$\left\{ \text{I}_{ec,i}^{min} + \left(\delta_{ec,i} \text{I}_{ec,i}^0 \right) \right\} \leq \text{I}_{ec,i}^{\hbar} \leq \left\{ \text{I}_{ec,i}^{max} + \left(\delta_{ec,i} \text{I}_{ec,i}^0 \right) \right\}. \tag{32}$$

11) Performance Metrics for Consumer ECC Reduction: The total energy consumption cost $(\mathbb{C}_{tot,i})$ is defined as the sum of total supplied energy to consumer LPD over a period and energy consumption cost/kWh, which can be expressed as:

$$\mathbb{C}_{tot,i} = \sum_{h=1}^{H-1} \left(\mathbb{C}_i^{\hbar} \mathcal{E}_{con,i}^{\hbar} \right) - \left\{ \mathbb{S}_{cost,i}^{\hbar} - \mathbb{B}_{cost,i}^{\hbar} \right\}. \tag{33}$$
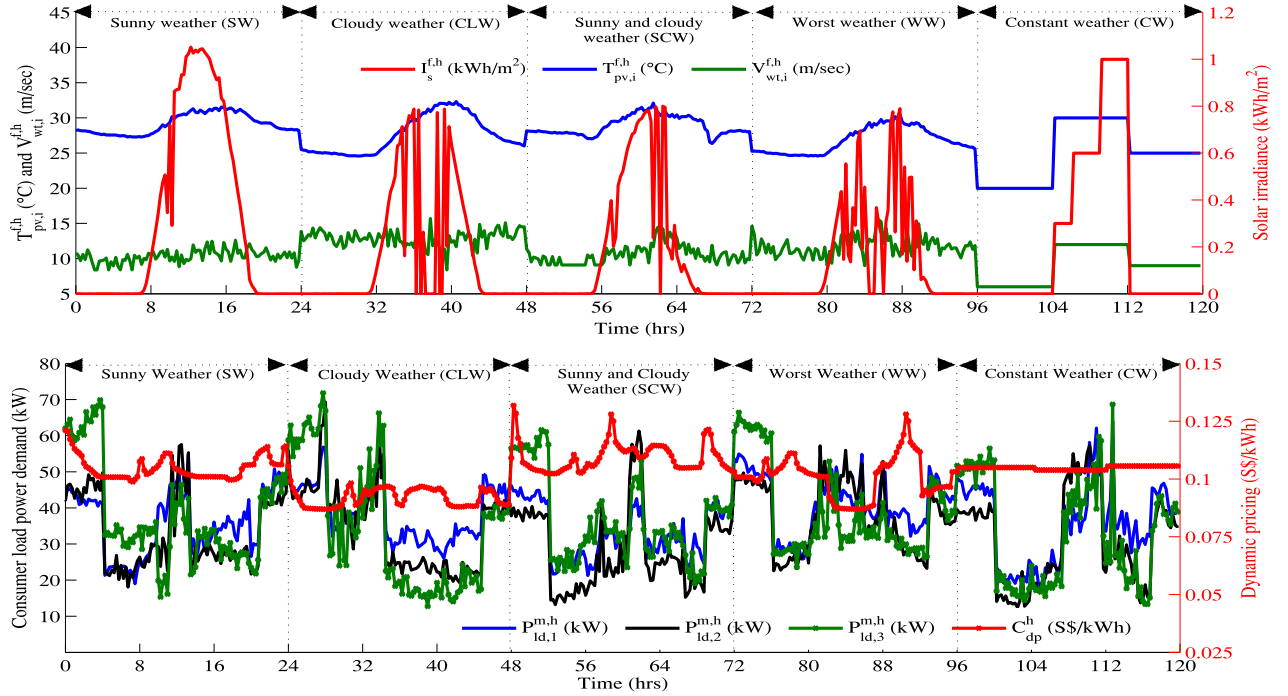
Fig. 5. Considered data for the simulation study (a) and (b) MG data of $I_s^{f,h}$, $T_{pv,i}^{f,h}$, and $V_{wt,i}^{f,h}$ and MG data of consumer $P_{ld,i}^{m,h}$ and $\mathbb{C}_{dp}^h$.

The performance metrics for consumer ECC savings ($\mathbb{C}_{sav,i}$) over the ODSS and CCRS can be expressed as:

$$\mathbb{C}_{sav,i} = \left(\mathbb{C}_{tot,i}^{ODSS} - \mathbb{C}_{tot,i}^{CCRS} \right) \left(\mathbb{C}_{tot,i}^{ODSS} \right)^{-1} \times 100. \quad (34)$$

The main advantages of the proposed EMS for the grid interconnected multi-microgrids are as follows: a) multiple MG operations; b) higher reliability of power supply rate; c) higher savings of energy consumption cost; d) lower diesel generator usage hours; and e) reduced consumer energy consumption cost while enabling surplus energy transfer to the grid and/or MGs through fuzzy-based P2P energy exchange algorithm with dynamic pricing. In this paper, we consider only the MG system operators, i.e., residential house operators. Inclusion of other stakeholders, for example, investors, could be an interesting aspect that can be explored in the future. The practical outcome of the proposed EMS for grid interconnected multi-microgrids is to reduce consumer energy consumption cost while enabling surplus energy exchange to grid and/or MGs through fuzzy-based P2P energy exchange algorithm with dynamic pricing. For example, the MG can be considered as a residential house. If multiple residential houses are interconnected with the grid, then the proposed EMS is capable to reduce the energy consumption cost of each residential house. If multiple residential houses are interconnected with the grid, then the proposed EMS is capable to reduce the energy consumption cost of each residential house. The $\mathcal{J}_1$ and $\mathcal{J}_2$ are the general version of ODSS and CCRS approach with an objective. Here, $\mathcal{J}_1$ can be any objective, if the system constraints, reliability index, and cost limits, are satisfied. Also, $\mathcal{J}_2$ can be any objective, if the system constraints, reliability index, energy index, cost margin, cost limit, and P2P limits are satisfied. That is, if the MG operator needs to minimize the consumer energy consumption cost, $\mathcal{J}_{cost}$ would be substituted for $\mathcal{J}_1$ in (24) and $\mathcal{J}_2$ in (24), respectively. The objective functions, i.e., (23) and (24), are formulated as a nonlinear programming problem, and there are many popular solvers that can be applied to solve this problem.

V. SIMULATION RESULTS AND DISCUSSION

In this section, the proposed EMS is demonstrated through the simulation study with real data of MG consumer LPD and weather data [5], [36]. The grid interconnected multi-microgrid models are implemented in the MATLAB environment and the cost reduction problem is solved with built-in tool. Many parameters affect MG consumer energy consumption cost reduction problem, which causes higher energy consumption cost of each MG at time slot $\hbar$. Mainly, the weather conditions play major role for the MG consumer LPD requirements. Hence, different types of weather conditions are considered to examine the proposed EMS, i.e., sunny weather (SW), cloudy weather (CLW), sunny and cloudy weather (SCW), worst weather (WW), constant weather (CW), to validate the MG consumer energy consumption cost reduction. To demonstrate the effectiveness of proposed CCRS, WW and CW conditions are considered. In CW, $I_s^{f,h}$, $T_{pv,i}^{f,h}$, and $V_{wt,i}^{f,h}$ are assumed to have three ranges: low, normal, and high, which is shown in Fig. 5. From 96 hrs to 104 hrs, $I_s^{f,h} = 0.25$ kW/m^2, $T_{pv,i}^{f,h} = 22$ °C, and $V_{wt,i}^{f,h} = 5$ m/sec, from 104 hrs to 112 hrs, $I_s^{f,h} = 0.45$ kW/m^2, $T_{pv,i}^{f,h} = 25$ °C, and $V_{wt,i}^{f,h} = 8$ m/sec, and from 112 hrs to 120 hrs, $I_s^{f,h} = 0.75$ kW/m^2, $T_{pv,i}^{f,h} = 28$ °C, and $V_{wt,i}^{f,h} = 10$ m/sec.

TABLE I
ENERGY BUYING AND SELLING COST RANGE IN S$/kWh

Range	$\mathbb{C}_{dp}^{\hbar}$	$\mathbb{C}_{pv,i}^{\hbar}$	$\mathbb{C}_{wt,i}^{\hbar}$	$\mathbb{C}_{e,i}^{\hbar}$	$\mathbb{C}_{d,i}^{h}$	$\mathbb{C}_{s,i}^{\hbar}$	$\mathbb{C}_{b,i}^{\hbar}$
Min.	0.09	0.03	0.01	-0.04	0.09	0.08	0.05
Max.	0.13	0.08	0.072	0.08	0.16	0.15	0.12

TABLE II
SIMULATION STUDY SPECIFICATIONS AND PARAMETER SETTINGS

Parameter	Unit	$i=1$	$i=2$	$i=3$
$m, \Delta h, H, I$	min.		15, 15, 480, 3	
$\eta_{e,i}, \eta_{c,i}, \eta_{d,i}$	%		96, 99, 97	
$SOC_{e,i}^{min}, SOC_{e,i}^{max}$	%		0.15, 0.9	
$\mathbb{C}_{d,1}^{ini}$	S$		3000	
$F_{con,i}$	liter/kWh		2.25	
$\mathbb{C}_{fc}$	S$/liter		0.51	
$\delta_{ec,i}, \mathrm{I}_{ec,i}^{0}$	-		0.04,0.01	
$P_{pv,i}^{max}, P_{wt,i}^{max}$	kW	22.2, 20	19.76, 20	18, 20
$P_{ld,i}^{max}, P_{d,i}^{max}$	kW	56.78, 20	67.73, 20	72.05, 20
$S_{e,i}$	kWh	96	104	112
$SOC_{e,i}^{in}$	%	75	46	29
$C_{e,i}^{max}, D_{e,i}^{max}$	1/hour	0.2, 0.2	0.15, 0.25	0.15, 0.2
$P_{e,i}^{max}\{c\}, P_{e,i}^{max}\{d\}$	kW	15, 16	16, 18	15, 18
$a_{e,i}, b_{e,i}, c_{e,i}, d_{e,i}$	-	0.56, 0.96, 0.63, 0.95	0.64, 0.87, 0.52, 0.68	0.35, 0.84, 0.72, 0.89

Fig. 6. Comparison of the network outputs with the training, validation, testing, and all data outputs.

The uncertainty in the weather condition is reflected in the objective function, i.e., both ODSS ($\mathcal{J}_1$) and CCRS ($\mathcal{J}_2$) approach. For example, the reliability index $\mathcal{R}_i^{\hbar}$ constraint of ith MG at time slot $\hbar$ has been used in both $\mathcal{J}_1$ and $\mathcal{J}_2$. Equality constraint, i.e., $\mathcal{R}_i^{\hbar} = 1$, has been used in $\mathcal{J}_1$ and inequality constraint, i.e., $\mathcal{R}_i^{min} \leq \mathcal{R}_i^{\hbar} \leq \mathcal{R}_i^{max}$, has been used in $\mathcal{J}_2$. Due to the uncertainty in the weather condition, the equality and inequality constraints might still be infeasible, which results in turning ON the ith MG diesel generator and/or buying energy from grid. The ith MG diesel generator energy cost, i.e., from 0.09 S$/kWh to 0.16 S$/kWh, and grid energy cost, i.e., from 0.09 S$/kWh to 0.13 S$/kWh, are given in Table I. The diesel generator and grid energy cost vary with respect to weather condition. Hence, the uncertainties in the weather condition would reflect consumer energy consumption cost of ith MG at time slot $\hbar$.

A. System Setup and Parameter Specifications of MGs

Fig. 5 shows the real data of MGs considered for the simulation study with different weather conditions. Here, the consumer LPD inputs, solar PV inputs, and wind turbine inputs are not shown, i.e., x_{in}^z. Also, dynamic pricing is used for the selling and buying cost of electricity generation and consumption. The selling and and buying cost minimum (Min.) and maximum (Max.) values are shown in Table I. The cost values are given in Singapore dollar per kWh, i.e., S$/kWh. The specifications and parameter settings are given in Table II.

Fig. 6 compares the RVFLN approach output with the training, validation, test, and target data. In the regression plot, the solid and dotted line indicates the best fit for the RVFLN output and the training data output. Here, the best fit in the training, testing, and validations overlap with the solid line. Also, the RVFLN approach is capable of fitting the relationship between inputs and outputs of the training data. Moreover, the predicted MG
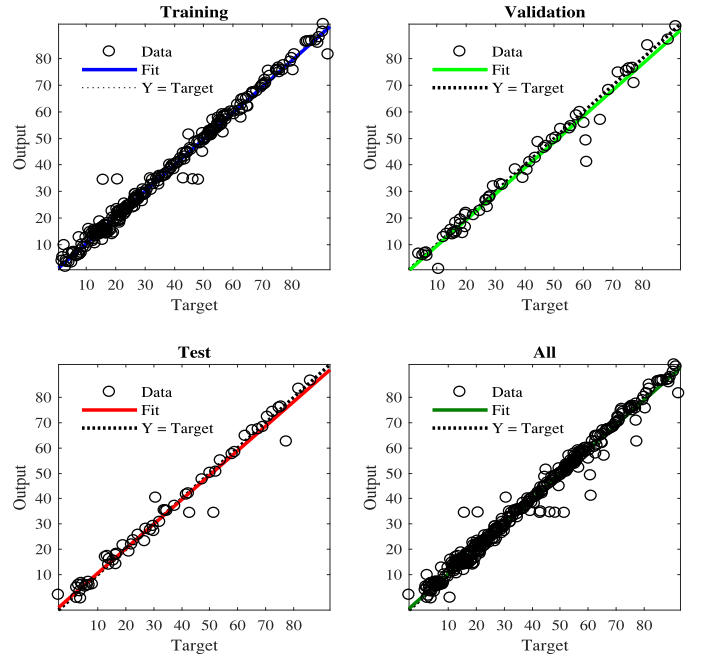
consumer load power demand tracks the target with the training data, testing data, and validation data. The MAPE is 2.96% with respect to the training, testing, and validation data. The accuracy of the RVFLN approach can be increased by adding more training information and by tuning the hidden layers and the learning rate within the network structure.

Fig. 7 compares the first MG predicted consumer LPD, solar PV output power, and wind turbine output power using RVFLN approach with measured values. Here, the scope of the paper is to predict the consumer LPD, solar PV output power, and wind turbine output power using RVFLN approach for future time slot. Hence, the output of the RVFLN approach is compared with the measured data of grid interconnected multi-microgrids. The predicted MG consumer load power demand MAPE for first MG is 2.91%, second MG is 2.79%, and third MG is 3.00%. The accuracy of the predicted consumer LPD depends on total number of layers for training and testing dataset. The training and testing dataset total number of layers are 123 and 21 for first MG, 120 and 20 for second MG, and 123 and 34 for third MG. In addition, the training and testing dataset mean absolute error is 2.76% and 3.41% for first MG, 3.67% and 4.38% for second MG, and 4.04% and 5.25% for third MG.

Fig. 8 shows the simulation results of ODSS approach such as selling power, DGs power, ESS charging/discharging power, diesel generator power, and buying power of grid and/or each MG. Here, the deficit power, solar PV power, wind turbine power, and the consumer LPD of each MG are not shown. If deficit power is greater than MG consumer LPD and ESS state-of-charge is lower, then the ODSS approach should decide to turn ON the diesel generator or buy energy from grid. In Fig. 8, the $P_{d,2}^h$ is greater than zero and $P_{b,2}^{\hbar}$ is equal to zero, which
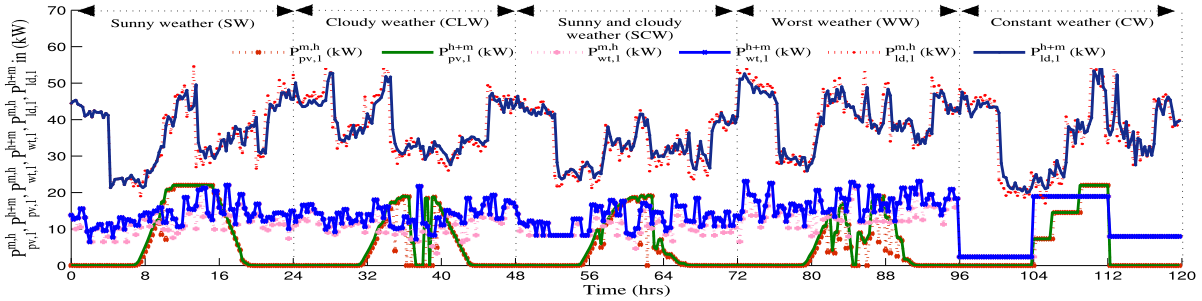
Fig. 7.   Compares the predicted consumer LPD, solar PV output power, wind turbine output power of MG-1 with measured values.
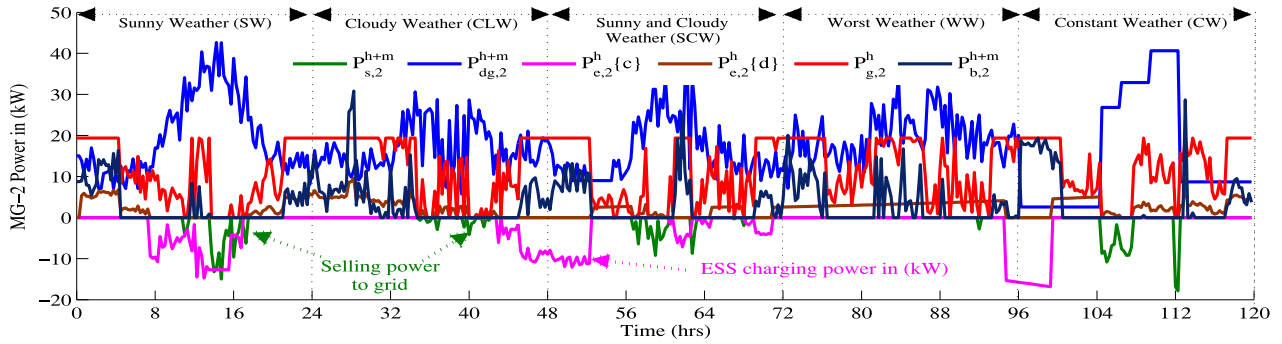

Fig. 8.   ODSS simulation results for $\alpha = 0.75$ of MG-2: $P^{\hbar}_{s,2}$, $P^{\hbar}_{dg,2}$, $P^{h}_{e,2}\{c\}$, $P^{h}_{e,2}\{d\}$, $P^{h}_{d,2}$, and $P^{\hbar}_{b,2}$.
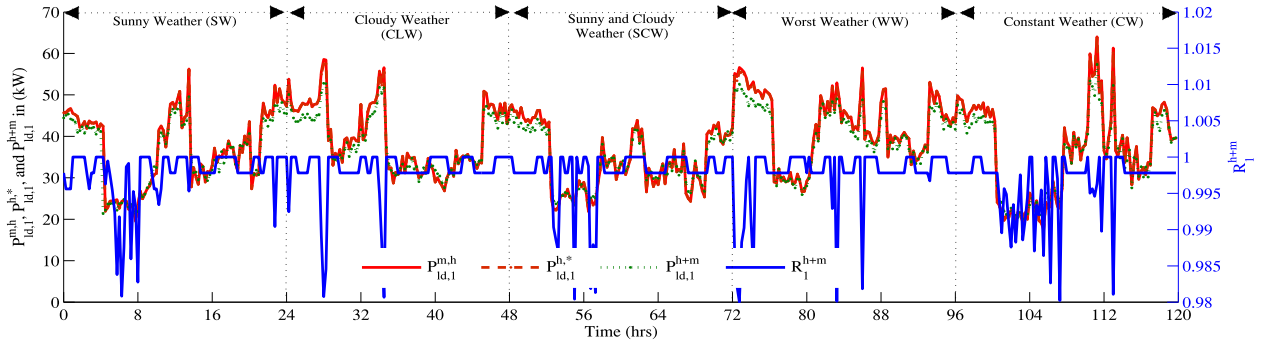
Fig. 9.   CCRS simulation results for $\alpha = 0.75$ of MG-1: compare the $P^{m,h}_{ld,1}$, $P^{\hbar,*}_{ld,1}$, $P^{\hbar}_{ld,1}$, and $\mathcal{R}^{\hbar}_{1}$.

indicates that the diesel generator power generation cost is lower than the energy buying cost from grid.

Fig. 9 shows the simulation results for the proposed CCRS with $\alpha = 0.75$, which compare the MG consumers actual LPD, predicted consumer LPD, reference consumer LPD, and reliability index of MG-3. The proposed CCRS maintains the MG consumer energy consumption cost within the threshold limits and the amount of LPD requirements are reduced based on the consumer energy consumption cost margin. The proposed CCRS predicts and checks the MG consumer LPD and the constraints. If constraints are satisfied, then the proposed CCRS reduces the MG consumer energy consumption cost using the fuzzy-based P2P energy exchange algorithm with dynamic pricing, which

maintain the consumer energy consumption cost margin within the limits.

Fig. 10 shows the simulation results of the MG consumer energy consumption cost for ODSS, CCRS, and the conventional approach, i.e., non-linear programming, with different objective balancing variable ($\alpha = 0.25$ and $\alpha = 0.75$). In the ODSS approach ($\alpha = 0.25$ and $i = 1$), the total energy consumption cost considering SW, CLW, SCW, WW, and CW are 92.5S\$, 89.13S\$, 90.83S\$, 97.81S\$, and 91.81S\$, respectively. In the CCRS approach ($\alpha = 0.25$ and $i = 1$), the total energy consumption cost for SW, CLW, SCW, WW, and CW are 87.11S\$, 94.01S\$, 95.35S\$, 103.91S\$, and 79.7S\$, respectively. In the conventional approach ($\alpha = 0.25$ and $i = 1$), the total

TABLE III
SUMMARY OF THE SIMULATION STUDY FOR THE MG CONSUMER ENERGY CONSUMPTION COST REDUCTION

α	Items	Type	i = 1					i = 2					i = 3				
			SW	CLW	SCW	WW	CW	SW	CLW	SCW	WW	CW	SW	CLW	SCW	WW	CW
	$\mathcal{E}_{con,i}$	ODSS	990.42	1107.48	982.09	1194.10	1001.19	985.04	977.36	842.49	1048.11	913.85	1128.39	1027.48	1046.49	1098.15	979.85
	(kWh)	CCRS	959.87	1123.11	978.41	1154.69	920.23	914.57	900.16	776.28	1017.14	868.68	1121.89	966.49	975.17	1145.26	887.08
		Conv.	1004.40	1137.60	1009.66	1209.63	999.14	987.80	938.76	849.85	1001.65	909.09	1125.14	1026.89	1031.05	1099.27	952.13
	$\mathbb{C}_{tot,i}$	ODSS	92.50	89.13	90.83	97.81	91.81	85.40	78.26	77.95	90.79	77.69	101.28	77.61	98.28	94.00	83.97
0.25	($)	CCRS	87.11	94.01	95.35	103.91	79.70	79.79	74.03	73.84	86.18	74.97	106.90	71.21	94.22	99.36	79.88
		Conv.	92.50	93.40	95.88	103.89	89.19	85.90	76.15	79.69	85.83	77.86	104.09	76.64	98.18	94.75	83.56
	$\mathrm{M}^{\hbar}_{ecc,i}$	ODSS	Changing from H to VB					Changing from H to VB					Changing from H to VB				
		CCRS	Changing from H to VB					Changing from S to H					Changing from L to VB				
		Conv.	Changing from M to VB					Changing from H to VB					Changing from M to H				
	$\mathcal{E}_{sav,i}$ (%)		5.83	-5.48	-4.98	-6.24	13.19	6.56	5.41	5.27	5.07	3.51	-5.54	8.25	4.13	-5.70	4.87
	$\mathcal{E}_{con,i}$	ODSS	884.92	989.51	877.47	1066.90	894.54	880.11	873.25	752.74	936.47	816.51	1008.20	918.03	935.02	981.17	875.48
	(kWh)	CCRS	906.46	1060.63	923.98	991.31	869.04	863.69	850.08	733.09	960.55	820.35	1059.47	912.72	920.92	1031.03	837.72
		Conv.	922.56	1025.07	918.74	1065.12	934.70	941.65	878.90	787.49	948.51	892.09	1044.17	970.30	992.93	1036.28	908.00
	$\mathbb{C}_{tot,i}$	ODSS	103.53	99.75	101.66	109.47	102.75	95.58	87.59	87.24	101.61	86.95	113.36	86.86	109.99	105.21	93.98
0.75	($)	CCRS	89.60	101.49	98.08	98.15	89.27	82.07	76.14	75.95	88.65	77.11	119.85	74.71	96.91	101.69	82.16
		Conv.	99.46	100.62	101.87	107.44	101.77	95.93	83.50	86.49	95.13	89.41	117.77	85.63	110.69	106.55	93.35
	$\mathrm{M}^{\hbar}_{ecc,i}$	ODSS	Changing from L to B					Changing from M to VB					Changing from M to VB				
		CCRS	Changing from S to B					Changing from VS to B					Changing from L to B				
		Conv.	Changing from L to VB					Changing from M to VB					Changing from M to VB				
	$\mathcal{E}_{sav,i}$ (%)		13.45	-1.74	3.52	10.34	13.12	14.13	13.07	12.94	12.76	11.32	-5.73	13.99	11.89	3.34	12.57
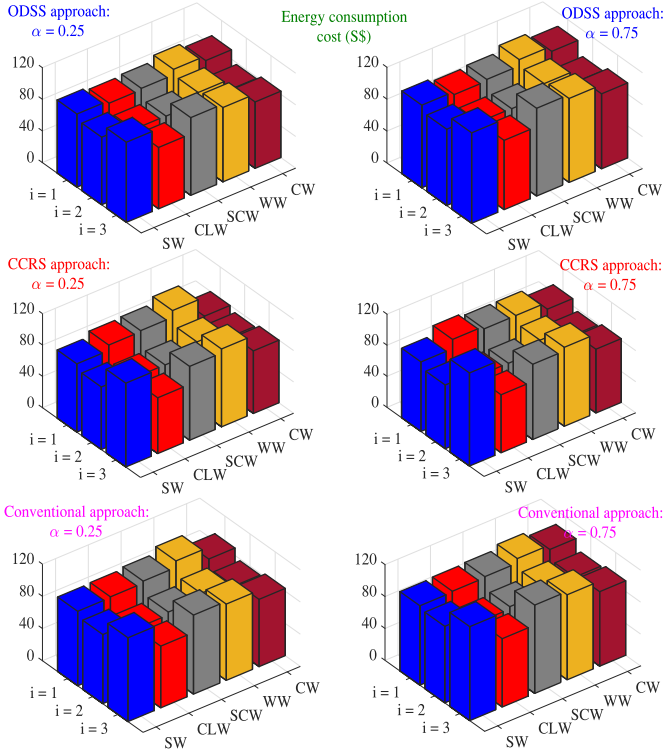
Fig. 10. Simulation results of the MG consumer energy consumption cost for ODSS (base line strategy), CCRS (proposed strategy), and conventional approach (non-linear programming) with $\alpha = 0.25$ (left) and $\alpha = 0.75$ (right).

energy consumption cost for SW, CLW, SCW, WW, and CW are 92.5S\$, 93.4S\$, 95.88S\$, 103.89S\$, and 89.19S\$, respectively. Here, the lower values of objective balancing variable provide higher preference to consumer energy consumption cost margin and lower preference to MG consumer energy consumption cost reduction. Hence, the proposed CCRS approach gives higher preference to ECC margin and lower preference to

MG consumer energy consumption cost reduction, i.e., CLW are 89.13S\$, 94.01S\$, 93.4S\$ for ($\alpha = 0.25$ and $i = 1$), respectively. In the ODSS approach ($\alpha = 0.25$ and $i = 3$), the total energy consumption cost for SW, CLW, SCW, WW, and CW are 101.28S\$, 77.61S\$, 98.28S\$, 94.0S\$, and 83.97S\$, respectively. In the CCRS approach ($\alpha = 0.25$ and $i = 3$), the total energy consumption cost for SW, CLW, SCW, WW, and CW are 106.9S\$, 71.21S\$, 94.22S\$, 99.36S\$, and 79.88S\$, respectively. In the conventional approach ($\alpha = 0.25$ and $i = 3$), the total energy consumption cost for SW, CLW, SCW,WW, and CW are 104.09S\$, 76.64S\$, 98.18S\$, 94.75S\$, and 83.56S\$, respectively. Hence, the proposed CCRS approach gives higher preference to MG consumer energy consumption cost reduction and lower preference to energy consumption cost margin, i.e., SCW are 98.28S\$, 94.22S\$, and 98.18S\$ for ($\alpha = 0.75$ and $i = 3$), respectively. Similarly, the MG consumer energy consumption cost for ODSS, CCRS, and the conventional approach with $\alpha = \{0.25, 0.75\}$ and $i = \{1, 2, 3\}$ are given in Table III. The proposed CCRS approach lowers the MG consumer ECC while maintaining the energy consumption margin within the threshold limit. As observed from Fig. 10, the proposed CCRS approach reduces energy consumption cost of the MG consumer, which is lower than both the ODSS and conventional approach.

Fig. 11 shows the simulation results of the MG consumer energy consumption cost based on the day-ahead prediction for the ODSS, CCRS, and conventional approach with $\alpha = 0.25$ and $\alpha = 0.75$. Here, the MG consumer energy consumption cost is shown based on the day-ahead prediction. The proposed EMS, i.e., both ODSS and CCRS, are illustrated with the conventional approach as shown in Fig. 11. In the ODSS approach, the total energy consumption cost for SW, CLW, SCW, WW, and CW are 113.36S\$, 86.86S\$, 109.99S\$, 105.21S\$, and 93.98S\$, respectively ($\alpha = 0.75$ and $i = 3$). In the CCRS approach, the total energy consumption cost for SW, CLW, SCW, WW, and CW are 119.85S\$, 74.71S\$, 96.91S\$, 101.69S\$, and 82.16S\$, respectively ($\alpha = 0.75$ and $i = 3$). In the conventional
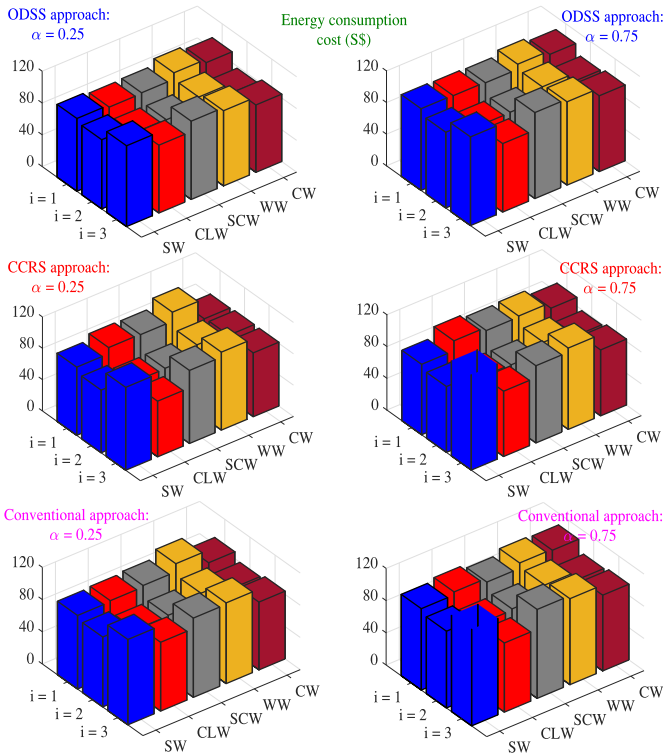
Fig. 11. Simulation results of the MG consumer energy consumption cost based on the day-ahead prediction for ODSS (base line strategy), CCRS (proposed strategy), and conventional approach (non-linear programming) with $\alpha = 0.25$ (left) and $\alpha = 0.75$ (right).

approach, the total energy consumption cost for SW, CLW, SCW, WW, and CW are 117.77S\$, 85.63S\$, 110.69S\$, 106.55S\$, and 93.35S\$, respectively ($\alpha = 0.75$ and $i = 3$). As observed from Fig. 11, the CCRS approach energy consumption cost is lower than the ODSS and conventional approach. From Fig. 10 and Fig. 11, the CCRS approach lowers the MG consumer energy consumption cost while maintaining the energy consumption cost margin within the threshold limit.

The summary of the simulation study is shown in Table III. To validate the proposed EMS, the simulation study is carried out with $\alpha = \{0, 0.25, 0.5, 0.75, 1\}$. Here, the summary of the simulation study is shown with $\alpha = 0.25$ and $\alpha = 0.75$. In the ODSS approach, the total energy consumption of the first MG on SW, CLW, SCW, WW, and CW are 990.42 kWh, 1107.48 kWh, 982.09 kWh, 1194.1 kWh, and 1001.19 kWh with $\alpha = 0.25$, respectively. The first MG consumer ECC margin varies from H to VB for ODSS with $\alpha = 0.25$. In the CCRS approach, the total energy consumption of first MG on SW, CLW, SCW, WW, and CW are 959.87 kWh, 1123.11 kWh, 978.41 kWh, 1154.69 kWh, and 920.23 kWh with $\alpha = 0.25$, respectively. In the conventional approach, the total energy consumption of the first MG on SW, CLW, SCW, WW, and CW are 1004.4 kWh 1137.6 kWh 1009.66 kWh 1209.63 kWh, and 999.14 kWh with $\alpha = 0.25$, respectively. In the CCRS approach, the total energy consumption of the first MG is lower than the ODSS and conventional approach with $\alpha = 0.25$. Here, the proposed CCRS approach reduces the consumer ECC while maintaining

the cost margin within threshold limits. Similarly, the second and third MG total energy consumption on different weather conditions are shown in Table III. At $\alpha = 0.75$ for the SW condition, the MG total energy consumptions are 884.92 kWh, 880.11 kWh, and 1008.2 kWh for the ODSS approach. Also, each MG consumer ECC margin for ODSS, CCRS, conventional approach on different weather conditions are shown in Table III. The first MG consumer ECC margin varies from L to B for the ODSS approach with $\alpha = 0.75$, where the lower values denote higher ECC margin and higher values denote lower ECC margin. In Table III, the negative sign indicates that the proposed CCRS supplied extra energy to maintain the MG consumer ECC margin, which is compared with the ODSS approach. In first MG, the total energy savings with $\alpha = 0.25$ on SW, CLW, SCW, WW, and CW are 5.83%, -5.48%, -4.98%, -6.24%, and 13.19%, respectively. The first MG consumer ECC margin for the proposed CCRS lies from S to B with $\alpha = 0.75$, which indicates that the proposed CCRS maintains the MG consumer ECC margin within the threshold limits. The total energy savings of the first MG with $\alpha = 0.75$ on SW, CLW, SCW, WW, and CW are 13.45% -1.74% 3.52% 10.34% 13.12%, respectively. The proposed CCRS is capable of lowering MG consumer ECC up to 14.13% while maintaining the MG consumer energy consumption margin within the threshold limits.

VI. CONCLUSION

This paper designs and develops an EMS to reduce consumer ECC while maintaining consumers ECC margin within the threshold limits by deciding the surplus energy exchange to grid and/or interconnected multi-microgrids. The proposed EMS relies on fuzzy-based P2P energy exchange algorithm with dynamic pricing. In this context, RVFLN approach has been used to predict the consumer LPD and DGs behaviors for future time slot. Furthermore, ESS charging/discharging energy control and diesel generator turned ON strategies has been developed based on the MGs deficit power. Also, consumer LPD reduction strategy has been developed based on the consumer ECC margin and energy consumption index. Then, an EMS has been implemented that includes both ODSS, which was the baseline strategy, and CCRS, which was the MG consumer energy consumption cost reduction strategy based on the future time slot values. The developed ODSS supplies the required LPD and saves consumer ECC based on the actual information. The proposed CCRS is capable of lowering MG consumer ECC up to 14.13% with MGs prediction models and surplus energy transfer to grid and/or MGs through fuzzy-based P2P energy exchange algorithm with dynamic pricing and concurrently controlling ESS energy as well as reducing diesel generator operating hours.

REFERENCES

[1] S. A. Arefifar, M. Ordonez, and Y. A. I. Mohamed, "Energy management in multi-microgrid systems-development and assessment," *IEEE Trans. Power Syst.*, vol. 32, no. 2, pp. 910–922, Mar. 2017.

[2] B. Zhao *et al.*, "Energy management of multiple microgrids based on a system of systems architecture," *IEEE Trans. Power Syst.*, vol. 33, no. 6, pp. 6410–6421, Nov. 2018.

[3] B. V. Solanki, A. Raghurajan, K. Bhattacharya, and C. A. Cañizares, "Including smart loads for optimal demand response in integrated energy management systems for isolated microgrids," *IEEE Trans. Smart Grid*, vol. 8, no. 4, pp. 1739–1748, Jul. 2017.

[4] D. Wu, F. Tang, T. Dragicevic, J. C. Vasquez, and J. M. Guerrero, "Autonomous active power control for islanded AC microgrids with photovoltaic generation and energy storage system," *IEEE Trans. Energy Convers.*, vol. 29, no. 4, pp. 882–892, Dec. 2014.

[5] K. Thirugnanam, S. K. Kerk, C. Yuen, N. Liu, and M. Zhang, "Energy management for renewable microgrid in reducing diesel generators usage with multiple types of battery," *IEEE Trans. Ind. Electron.*, vol. 65, no. 8, pp. 6772–6786, Aug. 2018.

[6] K. Rahbar, C. C. Chai, and R. Zhang, "Energy cooperation optimization in microgrids with renewable energy integration," *IEEE Trans. Smart Grid*, vol. 9, no. 2, pp. 1482–1493, Mar. 2018.

[7] Y. Liu, Y. Li, H. Xin, H. B. Gooi, and J. Pan, "Distributed optimal tie-line power flow control for multiple interconnected AC microgrids," *IEEE Trans. Power Syst.*, vol. 34, no. 3, pp. 1869–1880, May 2019.

[8] L. Chang, W. Zhang, S. Xu, and K. Spence, "Review on distributed energy storage systems for utility applications," *CPSS Trans. Power Electron. and Appl.*, vol. 2, no. 4, pp. 267–276, Dec. 2017.

[9] A. Hussain, V. Bui, and H. Kim, "A resilient and privacy-preserving energy management strategy for networked microgrids," *IEEE Trans. Smart Grid*, vol. 9, no. 3, pp. 2127–2139, May 2018.

[10] D. Sáez, F. Ávila, D. Olivares, C. Caãizares, and L. Marín, "Fuzzy prediction interval models for forecasting renewable resources and loads in microgrids," *IEEE Trans. Smart Grid*, vol. 6, no. 2, pp. 548–556, Mar. 2015.

[11] C. Ju, P. Wang, L. Goel, and Y. Xu, "A two-layer energy management system for microgrids with hybrid energy storage considering degradation costs," *IEEE Trans. Smart Grid*, vol. 9, no. 6, pp. 6047–6057, Nov. 2018.

[12] N. Rezaei, A. Ahmadi, A. H. Khazali, and J. M. Guerrero, "Energy and frequency hierarchical management system using information gap decision theory for islanded microgrids," *IEEE Trans. Ind. Electron.*, vol. 65, no. 10, pp. 7921–7932, Oct. 2018.

[13] H. Farzin, M. Fotuhi-Firuzabad, and M. Moeini-Aghtaie, "Role of outage management strategy in reliability performance of multi-microgrid distribution systems," *IEEE Trans. Power Syst.*, vol. 33, no. 3, pp. 2359–2369, May 2018.

[14] Z. Yi, W. Dong, and A. H. Etemadi, "A unified control and power management scheme for PV-battery-based hybrid microgrids for both grid-connected and islanded modes," *IEEE Trans. Smart Grid*, vol. 9, no. 6, pp. 5975–5985, Nov. 2018.

[15] M. R. Sandgani and S. Sirouspour, "Priority-based microgrid energy management in a network environment," *IEEE Trans. Sustain. Energy*, vol. 9, no. 2, pp. 980–990, Apr. 2018.

[16] D. O. Amoateng, M. Al Hosani, M. S. Elmoursi, K. Turitsyn, and J. L. Kirtley, "Adaptive voltage and frequency control of islanded multi-microgrids," *IEEE Trans. Power Syst.*, vol. 33, pp. 4454–4465, Jul. 2018.

[17] C. Zhang, J. Wu, Y. Zhou, M. Cheng, and C. Long, "Peer-to-peer energy trading in a microgrid," *Appl. Energy*, vol. 220, pp. 1–12, Feb. 2018.

[18] A. Paudel, K. Chaudhari, C. Long, and H. B. Gooi, "Peer-to-peer energy trading in a prosumer-based community microgrid: A game-theoretic model," *IEEE Trans. Ind. Electron.*, vol. 66, no. 8, pp. 6087–6097, Aug. 2019.

[19] D. Kiss, T. Hisakado, T. Matsushima, and O. Wada, "Peer-to-peer energy transfer by power gyrators based on time-variable-transformer concept," *IEEE Trans. Power Electron.*, vol. 34, no. 8, pp. 8230–8240, Nov. 2019.

[20] Y. Zhou, J. Wu, and C. Long, "Evaluation of peer-to-peer energy sharing mechanisms based on a multiagent simulation framework," *Appl. Energy*, vol. 222, pp. 993–1022, Jul. 2018.

[21] M. R. Alam, M. St-Hilaire, and T. Kunz, "Peer-to-peer energy trading among smart homes," *Appl. Energy*, vol. 238, pp. 1434–1443, Jan. 2019.

[22] C. Long, J. Wu, Y. Zhou, and N. Jenkins, "Peer-to-peer energy sharing through a two-stage aggregated battery control in a community microgrid," *Appl. Energy*, vol. 226, pp. 261–276, Sep. 2018.

[23] X. Wang, C. Wang, T. Xu, L. Guo, P. Li, L. Yu, and H. Meng, "Optimal voltage regulation for distribution networks with multi-microgrids," *Appl. Energy*, vol. 210, pp. 1027–1036, Jan. 2018.

[24] H. M. Ibrahim, M. S. El Moursi, and P. Huang, "Adaptive roles of islanded microgrid components for voltage and frequency transient responses enhancement," *IEEE Trans. Ind. Informat.*, vol. 11, no. 6, pp. 1298–1312, Dec. 2015.

[25] K. A. Alobeidli, M. H. Syed, M. S. El Moursi, and H. H. Zeineldin, "Novel coordinated voltage control for hybrid micro-grid with islanding capability," *IEEE Trans. Smart Grid*, vol. 6, no. 3, pp. 1116–1127, May 2015.

[26] P. A. Henríquez and G. A. Ruz, "Twitter sentiment classification based on deep random vector functional link," in *Proc. Int. Joint Conf. Neural Netw.*, Jul. 2018, pp. 1–6.

[27] C. Lork, Y. Zhou, R. Batchu, C. Yuen, and N. M. Pindoriya, "An adaptive data driven approach to single unit residential air-conditioning prediction and forecasting using regression trees," in *Proc. 6th Int. Conf. Smart Cities Green ICT Syst.*, Apr. 2017, pp. 67–76.

[28] N. Nikmehr and S. N. Ravadanegh, "Reliability evaluation of multi-microgrids considering optimal operation of small scale energy zones under load-generation uncertainties," *Int. J. Electr. Power Energy Syst.*, vol. 78, pp. 80–87, Jun. 2016.

[29] M. Sufyan, N. Abd Rahim, C. Tan, M. A. Muhammad, and S. R. S. Raihan, "Optimal sizing and energy scheduling of isolated microgrid considering the battery lifetime degradation," *PLoS ONE*, vol. 14, pp. 1–28, Feb. 2019.

[30] K. Thirugnanam, E. R. J. T. P., M. Singh, and P. Kumar, "Mathematical modeling of li-ion battery using genetic algorithm approach for V2G applications," *IEEE Trans. Energy Convers.*, vol. 29, no. 2, pp. 332–343, Jun. 2014.

[31] A. M. Pirbazari, M. Farmanbar, A. Chakravorty, and C. Rong, "Short-term load forecasting using smart meter data: A generalization analysis," *J. Processes*, vol. 8, pp. 1–22, Apr. 2020.

[32] K. Thirugnanam, T. P. E. R. Joy, M. Singh, and P. Kumar, "Modeling and control of contactless based smart charging station in V2G scenario," *IEEE Trans. Smart Grid*, vol. 5, no. 1, pp. 337–348, Jan. 2014.

[33] M. Braun, H. Altan, and S. Beck, "Using regression analysis to predict the future energy consumption of a supermarket in the UK," *Appl. Energy*, vol. 130, pp. 305–313, Oct. 2014.

[34] I. Korolija, Y. Zhang, L. Marjanovic-Halburd, and V. I. Hanby, "Regression models for predicting UK office building energy consumption from heating and cooling demands," *Energy and Building*, vol. 59, pp. 214–227, Apr. 2013.

[35] N. Fumo and M. A. R. Biswas, "Regression analysis for prediction of residential energy consumption," *J. Renew. Sustain. Energy Rev.*, vol. 47, pp. 332–343, Jul. 2015.

[36] NUS, "Geography weather station," May 2019, [Online]. Available: https://inetapps.nus.edu.sg/fas/geog/ajxdirList.aspx

Kannan Thirugnanam (Member, IEEE) received the B.Eng. degree in electronics and communication engineering from the Department of Electronics Communication Engineering, Government College of Engineering Bargur, Bargur, India, in 2005, the M.Eng. degree in power electronics and drives from the Department Electrical and Electronics Engineering, Alagappa Chettiar College of Engineering and Technology, Karaikudi, India, in 2009, and the Ph.D. degree in power electronics application to power systems from the Department of Electronics and Electrical Engineering, Indian Institute of Technology Guwahati, Guwahati, India, in 2014. He was an Assistant Professor with the National Institute of Technology Sikkim, Ravangla, India. He was a Research Fellow with Singapore University of Technology and Design, Singapore. He is currently a Postdoctoral Researcher with the Department of Electrical Engineering and Computer Science, Khalifa University of Science and Technology, Abu Dhabi, UAE. His research interests include renewable energy integration with grid, energy management of microgrid, solar thermal systems, contactless power transfers, power electronics, and power electronics applications in power systems.

Mohamed Shawky El Moursi (Senior Member, IEEE) received the B.Sc. and M.Sc. degrees from Mansoura University, Mansoura, Egypt, in 1997 and 2002, respectively, and the Ph.D. degree from the University of New Brunswick (UNB), Fredericton, NB, Canada, in 2005, all in electrical engineering. He was a Research and Teaching Assistant with the Department of Electrical and Computer Engineering, UNB, from 2002 to 2005. He joined McGill University as a Postdoctoral Fellow with the Power Electronics Group. He joined Vestas Wind Systems, Arhus, Denmark, in the Technology R&D with the Wind Power Plant Group. He was with TRANSCO, UAE, as a Senior Study and Planning Engineer. He is currently a Professor with the Department of Electrical and Computer Engineering, Khalifa University of Science and Technology- Masdar Campus, Abu Dhabi, UAE and seconded to a Professor Position with the Faculty of Engineering, Mansoura University, Mansoura, Egypt and currently on leave. He was a Visiting Professor with the Massachusetts Institute of Technology, Cambridge, Massachusetts, USA. His research interests include power system, power electronics, FACTS technologies, VSC-HVdc systems, microgrid operation and control, renewable energy systems (Wind and PV) integration and interconnections. He is currently an Editor for the IEEE TRANSACTIONS ON POWER DELIVERY, IEEE TRANSACTIONS ON POWER SYSTEMS, an Associate Editor for the IEEE TRANSACTIONS ON POWER ELECTRONICS, IEEE TRANSACTIONS ON SMART GRID, a Guest Editor for the IEEE TRANSACTIONS ON ENERGY CONVERSION, the Guest Editor-in-Chief for special section between IEEE TRANSACTIONS ON POWER DELIVERY and IEEE TRANSACTIONS ON POWER SYSTEMS, an Editor for the IEEE POWER ENGINEERING LETTERS, a Regional Editor for *IET Renewable Power Generation*, and an Associate Editor for *IET Power Electronics Journals*.

Vinod Khadkikar (Senior Member, IEEE) received the M.Tech. degree in power electronics, electrical machines and drive from the Indian Institute of Technology (IITD), New Delhi, India, in 2002 and the Ph.D. degree in electrical engineering from the Ecole de Technologie Superieure, Montreal, QC, Canada, in 2008. From December 2008 to March 2010, he was a Postdoctoral Fellow with the University of Western Ontario, London, ON, Canada. In 2010, he was a Visiting Faculty with the Massachusetts Institute of Technology, Cambridge, MA, USA. He is currently a Professor with the Department of Electrical Engineering and Computer Science, Khalifa University, Abu Dhabi, UAE. His research interests include applications of power electronics in distribution systems and renewable energy resources, grid interconnection issues, power quality enhancement, active power filters and electric vehicles. He is currently an Associate Editor for the IEEE TRANSACTIONS ON INDUSTRIAL ELECTRONICS, IEEE TRANSACTIONS ON INDUSTRY APPLICATIONS, and *IET Power Electronics*.

Hatem H. Zeineldin (Senior Member, IEEE) received the B.Sc. and M.Sc. degrees in electrical engineering from Cairo University, Giza, Egypt, in 1999 and 2002, respectively, and the Ph.D. degree in electrical and computer engineering from the University of Waterloo, Waterloo, ON, Canada, in 2006. He was with Smith and Andersen Electrical Engineering, Inc., North York, ON, USA, where he was involved in projects involving distribution system designs, protection, and distributed generation. He was a Visiting Professor with the Massachusetts Institute of Technology, Cambridge, MA, USA. He is currently with the Faculty of Engineering, Cairo University, and is on leave from the Khalifa University of Science and Technology, Abu Dhabi, UAE. His current research interests include distribution system protection, distributed generation, and micro grids. He is currently an Editor for the IEEE TRANSACTIONS ON ENERGY CONVERSION.

Mohamed Al Hosani (Senior Member, IEEE) received the B.Sc. degree in electrical engineering from the American University of Sharjah, Sharjah, UAE, in 2008, and the M.Sc. and Ph.D. degrees in electrical engineering from the University of Central Florida, Orlando, FL, USA, in 2010 and 2013, respectively. He was an Assistant Professor with the Department of Electrical and Computer Engineering, Khalifa University, Abu Dhabi, UAE, during 2014–2018, and a Visiting Assistant Professor with the Massachusetts Institute of Technology, Cambridge, MA, USA, during 2015–2016. He is currently the Department Manager of Demand Side Management (DSM), Abu Dhabi Distribution Company, Abu Dhabi, UAE. His research interests include demand side management, distributed generation protection and control, modeling and stability analysis of microgrid, and smart grid.